Prediction of the Power Losses of PWM Inverter Drives for Permanent Magnet Synchronous Motors

by

Jian Yang

Thesis submitted to the Faculty of the
Virginia Polytechnic Institute and State University
in partial fulfillment of the requirements for the degree of
Master of Science
in
Electrical Engineering

APPROVED:

Dr. Dan Y. Chen, Chairman

Dr. Fred C. Lee

Dr. Dusan Borojevic

September, 1995

Blacksburg, Virginia

Prediction of the Power Losses of PWM Inverter Drives for Permanent Magnet Synchronous Motors

by

Jian Yang

Committee Chairman: Dr. D. Y. Chen

Electrical Engineering

(Abstract)

A model is developed for predicting power losses for a hard-switching three-phase IGBT inverter drive for synchronous motor applications. For a given set of motor parameters, semiconductor device parameters and motor operating conditions, the various losses and the temperature rises of semiconductor junction can be predicted. All parameter values, semiconductor or motor, required to predict the losses are readily available from manufacturer's data sheet. Using this model, a number of IGBTs were evaluated for the suitability of synchronous motor applications. Conclusions of this evaluation are presented in the thesis. The model has been verified experimentally using both electrical power measurement and thermal measurement.

Acknowledgments

First of all, I would like to express sincere appreciation to my advisor, Dr. Dan Y. Chen for his guidance, patience and encouragement. Without his support and advice, I would have not been able to finish the program.

I would also like to thank Dr. Fred C. Lee and Dr. Dusan Borojevic for their time and effort for serving in my committee.

I am grateful to Motion Control Systems, Inc. and Virginia Center for Innovation Technology who provide fund for the project, and all professors, staffs, and colleagues of VPEC.

I want to thank my parents for their love, encouragement and support for the study.

Finally, I would like to thank my wife Anmin Li for her daily encouragement and emotional support. Without her support, I would not have been able to finish my graduate study.

Table of Contents

List of Figures

List of Tables

Chapter 1

Introduction

Permanent magnet synchronous motors driven by voltage-fed inverters are widely used in industrial servo applications. Synchronous motors feature high efficiency, compact size and ease of control. To control the motion of the motors, an adjustable-frequency-dc-to-three phase bridge inverter is normally used. An inverter consists of power semiconductor switches which are turned on and off to synthesize proper voltage and current to the motor. In recent years, insulated gate bipolar transistors (IGBT) are gaining wide acceptance for inverter applications particularly for 220-V and 440-V line input voltage. IGBT device rating up to 1400 V 600 A are commercially available nowadays, and high power devices are being developed.

Inverter power losses are major concern for an engineer working in motor drive field. The losses not only affect the overall system efficiency, but also the size and the ventilation required of the heat sink. Therefore, the capability to predict inverter power losses is a key part of the overall design capability. The main focus of the thesis work is to develop a computer-aided tool for predicting inverter power losses and the semiconductor device temperature rise associated with it. Only IGBT-based inverter drive for synchronous motor is considered. A conventional DC-to-three phase hard-switching

voltage-fed inverter is the focus of the effort. Commonly-used sine-wave pulse-width modulation scheme is used in the inverter control.

Models for calculating inverter power losses have been reported in literature[4]. However, the model does not take into consideration the operation of the motor nor have these models been extensively verified. Some of the models are used in this thesis as a starting point to develop a computer-aided program for predicting the power losses of various device for synchronous motors operating in three different modes: motoring, regeneration and stall. The input to this program consists of description of the motor parameters, the semiconductor device parameters, and motor operating conditions. The output of the program consists of the various losses associated with the inverter and the temperature rise of the devices. The program outputs have been verified experimentally. Using this capability, an investigation of existing IGBT loss characteristics for synchronous motor applications was conducted and conclusions are presented.

The thesis is organized as follows. Chapter 2 briefly describes the operation of an inverter of a permanent magnet synchronous motor operating in motoring, regenerating, and stalled mode. From the description of operation, duty cycle conduction of the various switches in the inverter can be found, which is the first step to find out device conduction losses covered in Chapter 3. Device models and equations for calculating the power loses are presented in Chapter 3. This include three modes of operation, the motoring mode, the regenerating mode and the stalled mode. Formulas for calculating the device temperature rise are also discussed in this chapter. Chapter 3 contains the procedure of power losses

calculations of an inverter in three modes. In Chapter 4, experimental verification of the power losses prediction is discussed. Two methods were used for power loss measurement. One uses thermal measurement, the other uses electrical measurement. Chapter 5 evaluates the performances of the second generation IGBTs and the third generation IGBTs for existing systems. Chapter 6 draws a conclusion of the thesis and describes possible future studies.

Because of a number of symbols used in the discussion, a list of symbols is given in the section Appendix.

Chapter 2

Operation of Synchronous Motor with PWM Inverter

A briefly review of the operation of the PWM-controlled synchronous motor provides foundation for inverter losses prediction. For a permanent magnet brushless motor where the magnets are mounted on the rotor surface, the effect of saliency and armature reaction is negligible due to large effective air gap. Therefore, the resultant main field is nearly equal to the rotor field. In order to produce the largest torque for a given stator current, an efficient operation is achieved by stator current control so that the stator current contains only a quadrature component when expressed in the reference frame fixed to the rotor [1] [2].

Fig. 2.1 shows the overall block diagram of a brushless servomotor drive system with sinusoidal waveforms. The motor rotor position is sensed by means of a position sensor such as a resolver. The speed signal ω which can be from the position sensor circuit is regulated at its reference ω^*. The amplified error between ω^* and ω is multiplied with the sinusoidal signal from a prestored lookup table in a read-only memory (ROM), the current request i_a^*, i_b^* and i_c^* are generated. The motor current is forced to follow the requested current by the current feedback loop. With a comparator for each phase, which compares a sine and a triangular waves, the triangular carrier voltage V_t intercepts V_{ref}. Each comparator outputs a high level whenever the instantaneous input reference level

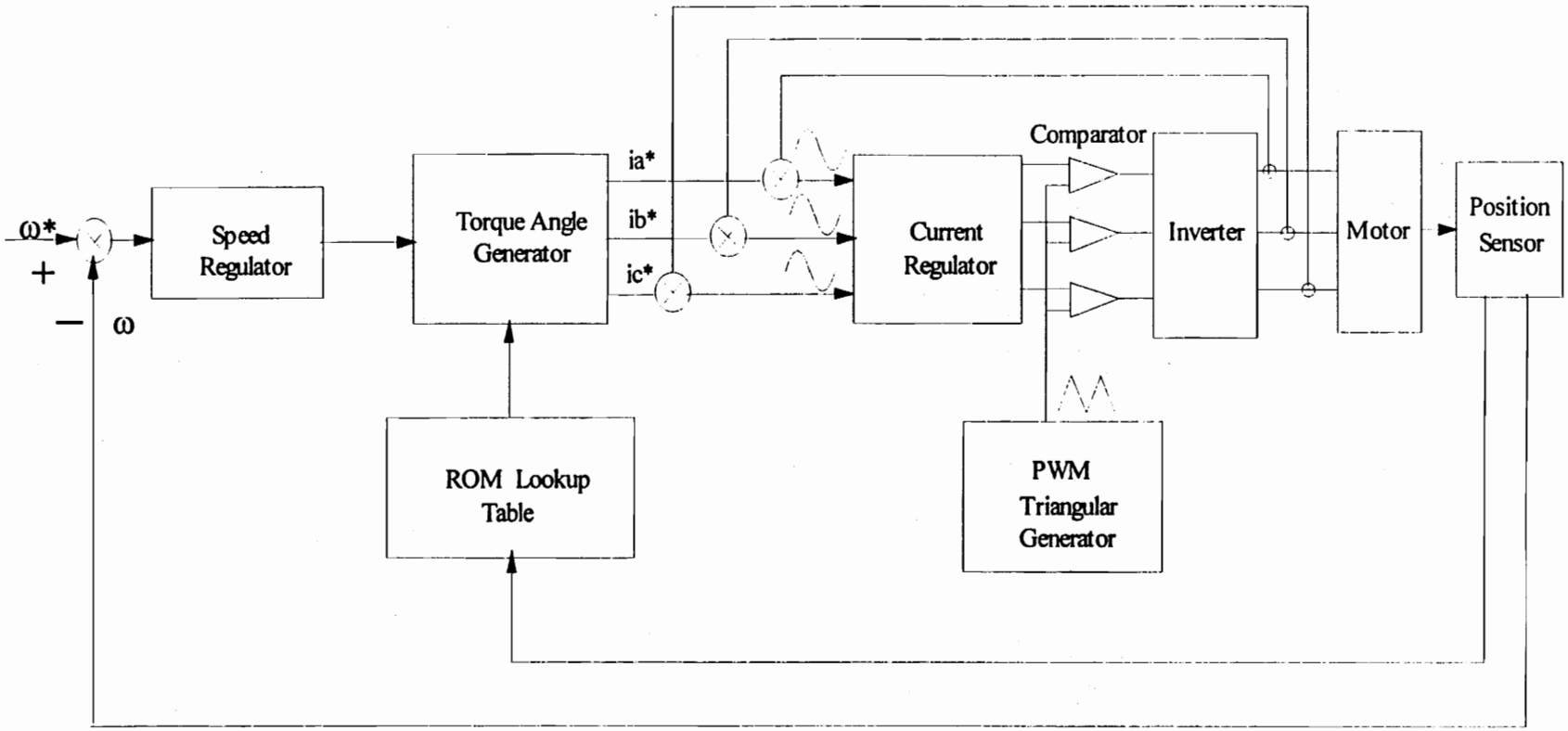

Fig. 2.1 Block Diagram of the System

exceeds the carrier voltage level and a low level when the reference is exceeded by the carrier voltage, resulting in PWM switching waveform. The comparator outputs are used to generate gate drive signals for the inverter semiconductor switches. As a result, the inverter phase voltage waveform V_a reproduces the comparator output voltage whose fundamental V_{a1} has the same frequency and the same phase as the corresponding reference signal V_{ref} [4] i.e.,

$$\frac{V_{a1}}{E_d/2} = \frac{V_{ref}}{V_t} \qquad (2.1)$$

Where V_t is the amplitude of the triangular carrier voltage V_t, V_{a1} is the amplitude of the fundamental V_{a1} and V_{ref} is the amplitude of reference signal V_{ref}.

Three modes of motor operation are discussed in conjunction with an inverter in this section: motoring mode, regenerating mode and stalled mode.

2.1 Motoring Mode of Operation

Figure 2.2 shows typical waveforms of the inverter when the motor is operating in the motoring mode, where V_a is the phase voltage (with respect to the center point of the input DC voltage source E_d), V_{a1} is the fundamental component of V_a, i_a is the fundamental of the motor phase current, and φ is the angle between the two fundamentals

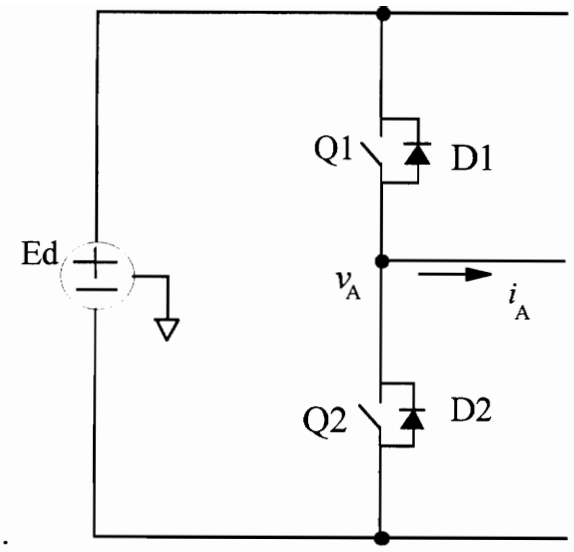

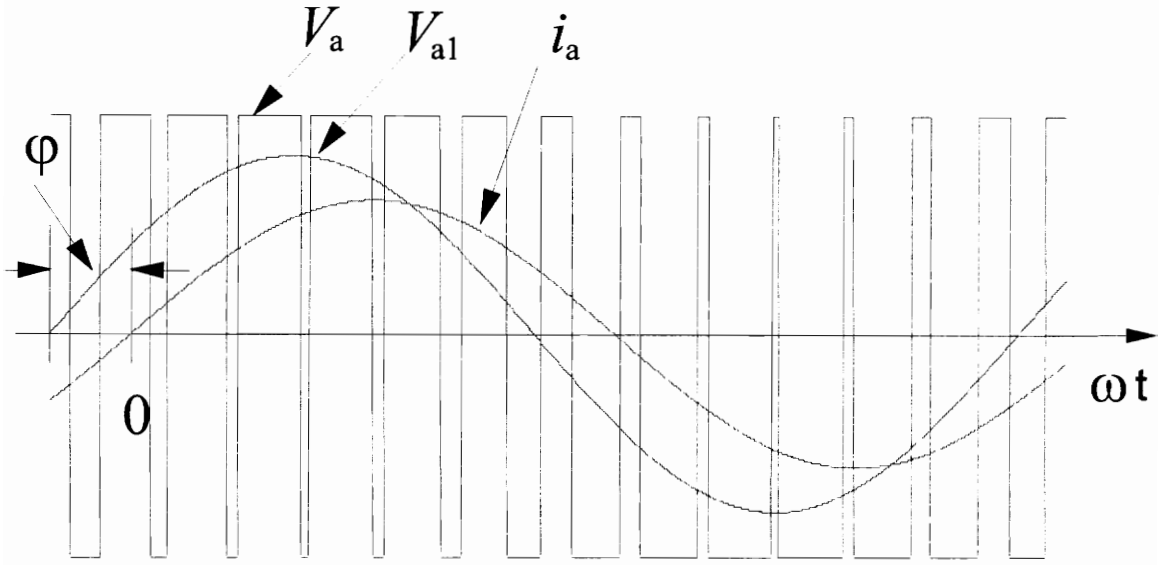

Fig. 2.2 Typical Waveforms of Inverter Operating in Motoring Mode

V_{a1} and i_a. Notice in Figure 2.2 that (Q1, D2) pair conducts when $i_a > 0$, and (Q2, D1) pair conducts when $i_a < 0$. Also, IGBTs conduct with larger period of time than diodes do. This is typical of motoring mode operation. The magnitude of phase angle φ depends on motor inductance and motor phase current. Figure 2.3 shows the equivalent circuit and the phasor diagram representing a synchronous motor operation, where $\mathbf{V_{a1}}$ is fundamental phase voltage, $\mathbf{I_a}$ is fundamental phase current, $\mathbf{V_f}$ is motor back EMF voltage per phase, R_s is motor phase resistance and L_s is motor phase inductance. Notice that the phase current $\mathbf{I_a}$ is always in phase with $\mathbf{V_f}$ in a proper synchronous motor operation. It can be obtained, by using Figure 2.3 (b) and trigonometry, that the following two equations:

$$\varphi = \tan^{-1}\frac{\omega L_s I_a}{V_f + R_s I_a} \qquad (2.2)$$

$$V_{a1} = \frac{V_f + R_s I_s}{\cos\varphi} \qquad (2.3)$$

These two equations will be used in Chapter 3 to determine the switch conduction duty cycle to predict switch conduction loss.

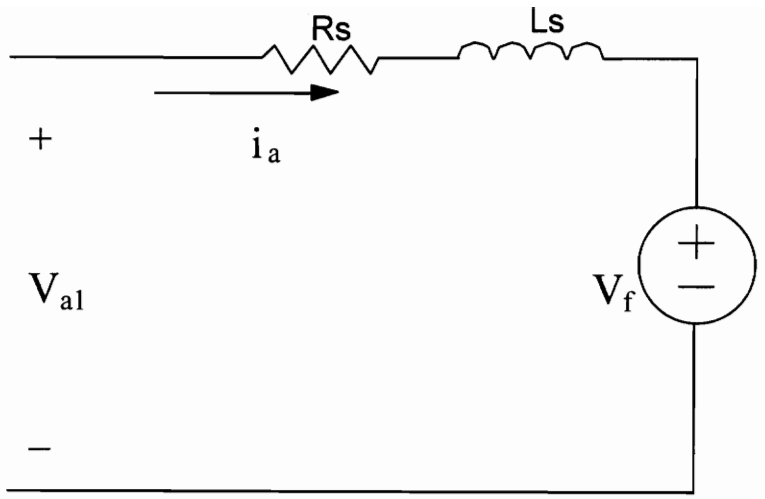

(a)

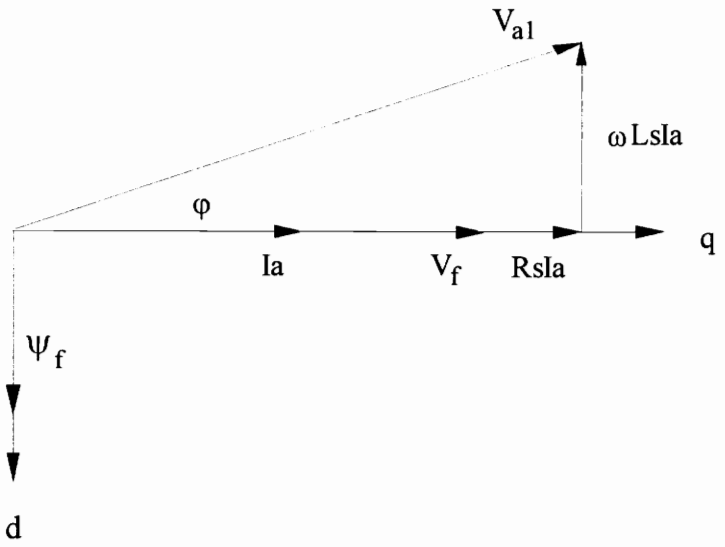

(b)

Fig. 2.3 (a) Phase Equivalent Circuit of Synchronous Motor in Motoring Mode

(b) Phasor Diagram for Brushless Motor Operating in Motoring Mode

2.2 Regenerating Mode

When a motor decelerates or reverses its direction, the motor is operated in the regenerating mode and the kinetic energy associated with the inertia of the motor and its load is recovered to the DC bus. With the uncontrolled rectifier-supplied DC bus, because the power can not flow back to the utility, it charges the input filter capacitor and raises the DC bus voltage. A dynamic braking resistor, which can be switched on across the filter capacitor, is often used to dissipate the energy to prevent bus overvoltage. As operated in the rectifier mode, the phase current $\mathbf{I_a}$ is 180° out of phase with $\mathbf{V_f}$ as shown in Figure 2.4(b), resulting in the power flowing from the motor to the DC bus of the inverter.

Figure 2.5 shows typical waveforms in this mode, where V_a, V_{al} and i_a are defined as the same as in figure 2.2, and φ is the angle between the V_{al} and V_f.

Assuming the inertia of the motor and its load large enough, meaning that the steady-state operation of this mode exists, the following two equations can be obtained referring to figure 2.4 (b)

$$\varphi = \tan^{-1}\frac{\omega L_s I_a}{V_f - R_s I_a} \qquad (2.4)$$

$$V_{al} = \frac{V_f - R_s I_s}{\cos\varphi} \qquad (2.5)$$

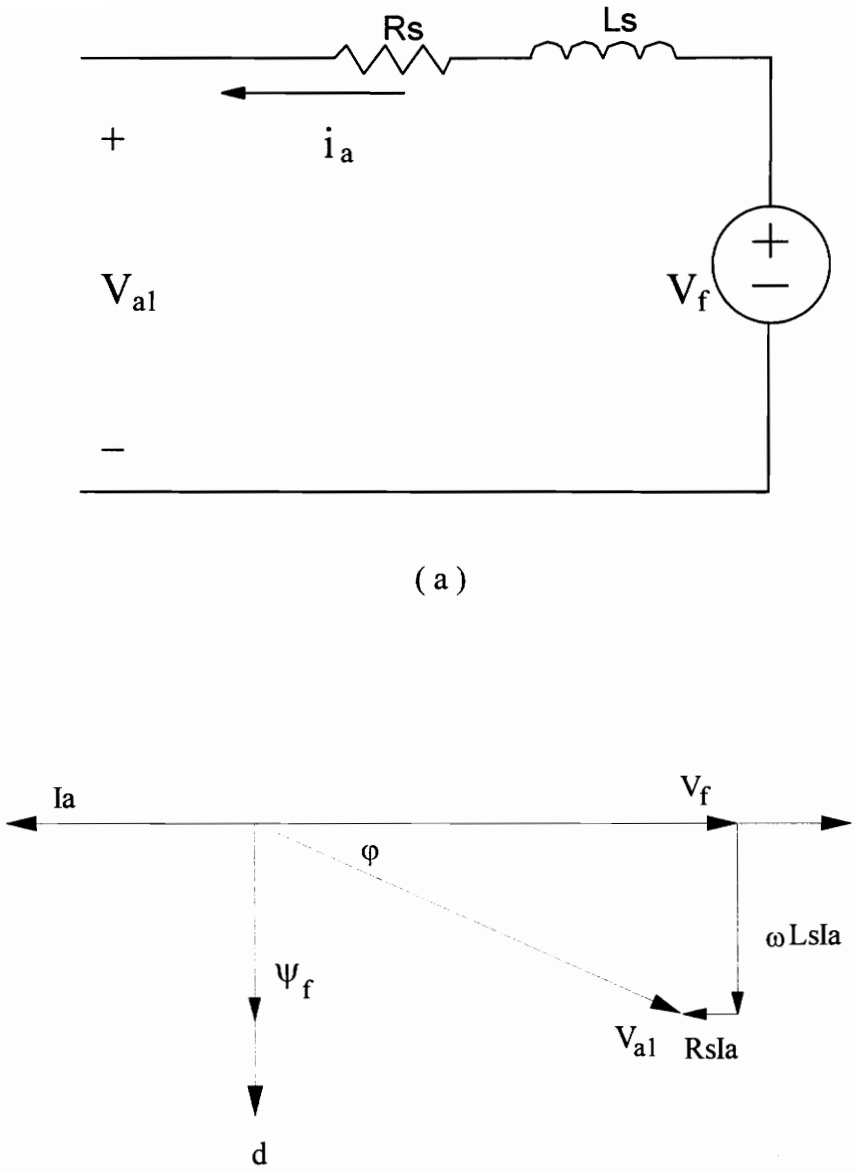

Fig. 2.4 (a) Phase Equivalent Circuit of Synchronous Motor in Regenerative Mode

(b) Phasor Diagram for Brushless Motor Operating in Regenerative Mode

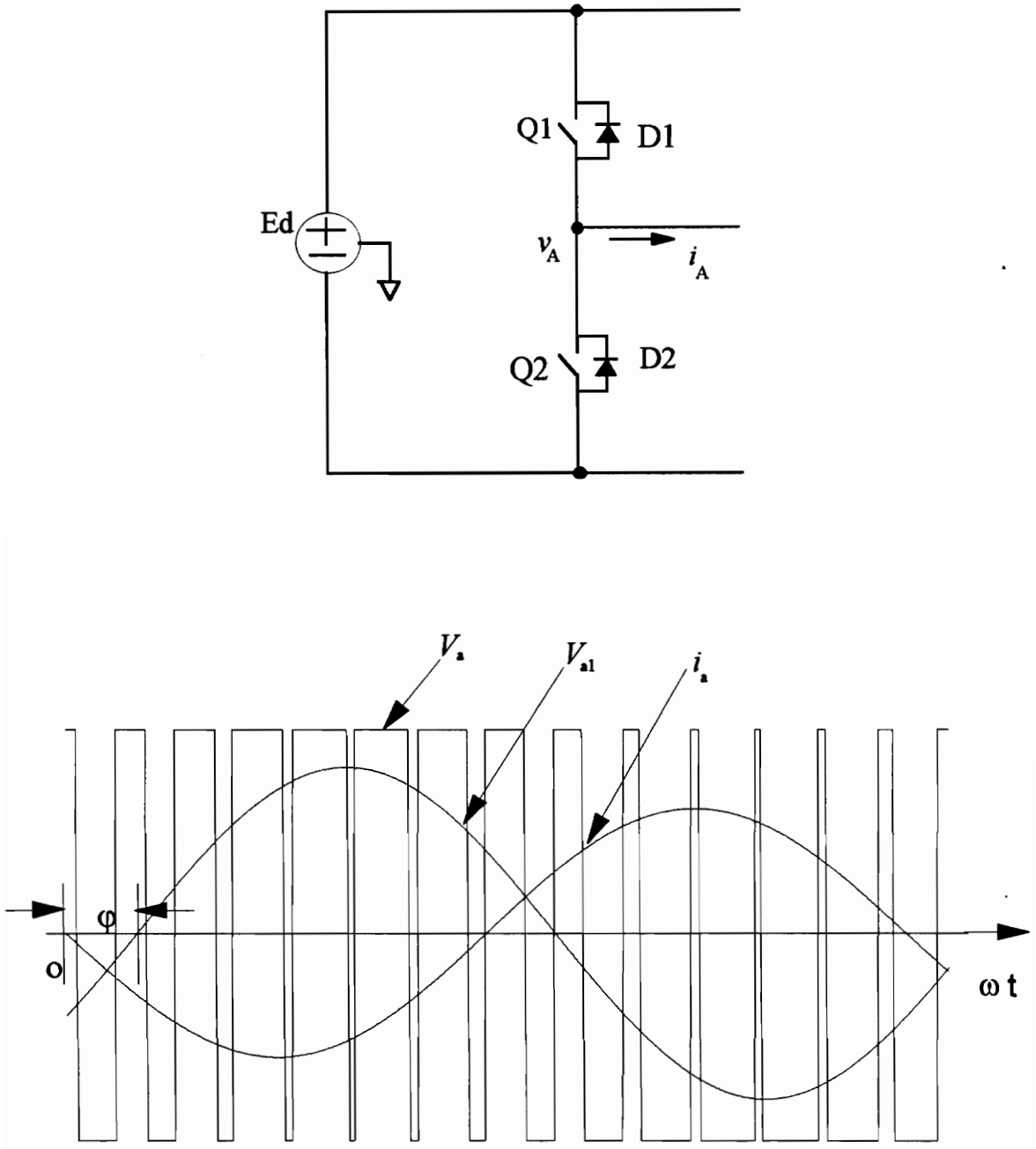

Fig. 2.5 Typical Waveforms of Inverter Operating in Regenerative Mode

These two equations will be used in Chapter 3 to determine switch conduction duty cycle when the motor is operating in the regenerating mode.

2.3 Stalled Mode of Operation

When a motor is stalled, all of the three phase stator current are DC current. The current magnitude of each phase depends on the stalled position of the rotor with respect to the stator. Fig. 2.6 shows an example of phase current at stalled condition, where $I_a + I_b + I_c = 0$. Under this condition, Only half of the inverter devices are used , i.e. (Q1,D2) for conducting I_a, (Q4,D3) for I_b and (Q6,D5) for I_c. The worst condition, in terms of heating of device, occurs when one of the three phases current is the inverter current limit.

In a stalled condition, the motor back EMF V_f is zero, and the motor average winding inductive voltage drop is also zero. Therefore, the phase current is the average voltage divided by winding resistance R_s. Since R_s is normally small, the DC average resistive voltage drop is also very small as indicated in Figure 2.6. This means that the switch duty cycle is approximately 50%. This effect will be used in the prediction of the switch losses associated with stalled mode of operation.

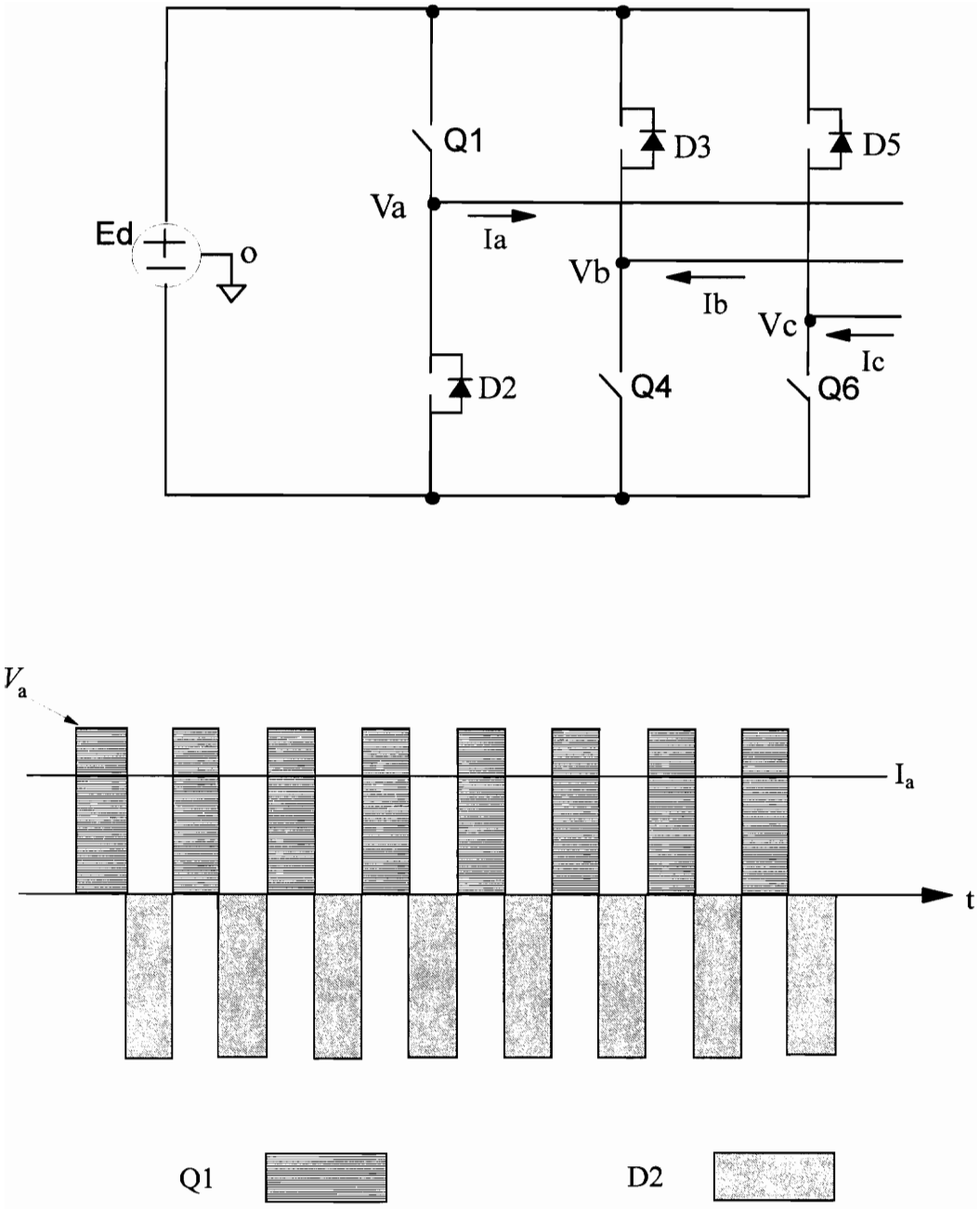

DC Average Phase Voltage $< Va > \approx 0$

Fig. 2.6 An Example of Inverter Phase Voltage and Current (Phase A) of Stalled Mode Operation

2.4 Effect of Dead Time on Inverter Performance

In the previous discussion, the switches were assumed to be ideal, which means that the two switches in an inverter leg are capable of turning on and off simultaneously. In practice, however, when a switch in the inverter leg is turned off, the turn on of the other switch in the leg is delayed by a time t_d (normally referred as dead time) to avoid cross conduction through the leg due to the finite switching time with any switches. In a particular design, the choice of dead time depends on how fast the switch turn off. Normally it is chosen large enough to avoid cross conduction in an inverter but should not be too large. A provision of large dead time reduces the fundamental of the inverter output voltage waveform.

As shown in Figure 2.7, since both switches are off during the dead time, the inductive current must flow through diode (D1 or D2) depending upon which direction the phase current (i_A) flows.

It can be seen from Figure 2.7 that the effective output phase voltage is averagely reduced by the amount $\frac{t_d}{T_s}E_d$ compared to the ideal condition for each switching period. Therefore, the maximum output phase voltage is $\frac{E_d}{2}-\frac{t_d}{T_s}E_d$ in the motoring mode if dead time effect is included. Table 2.1 gives the percentage reduction of maximum output voltage for different combination of dead time and PWM frequency.

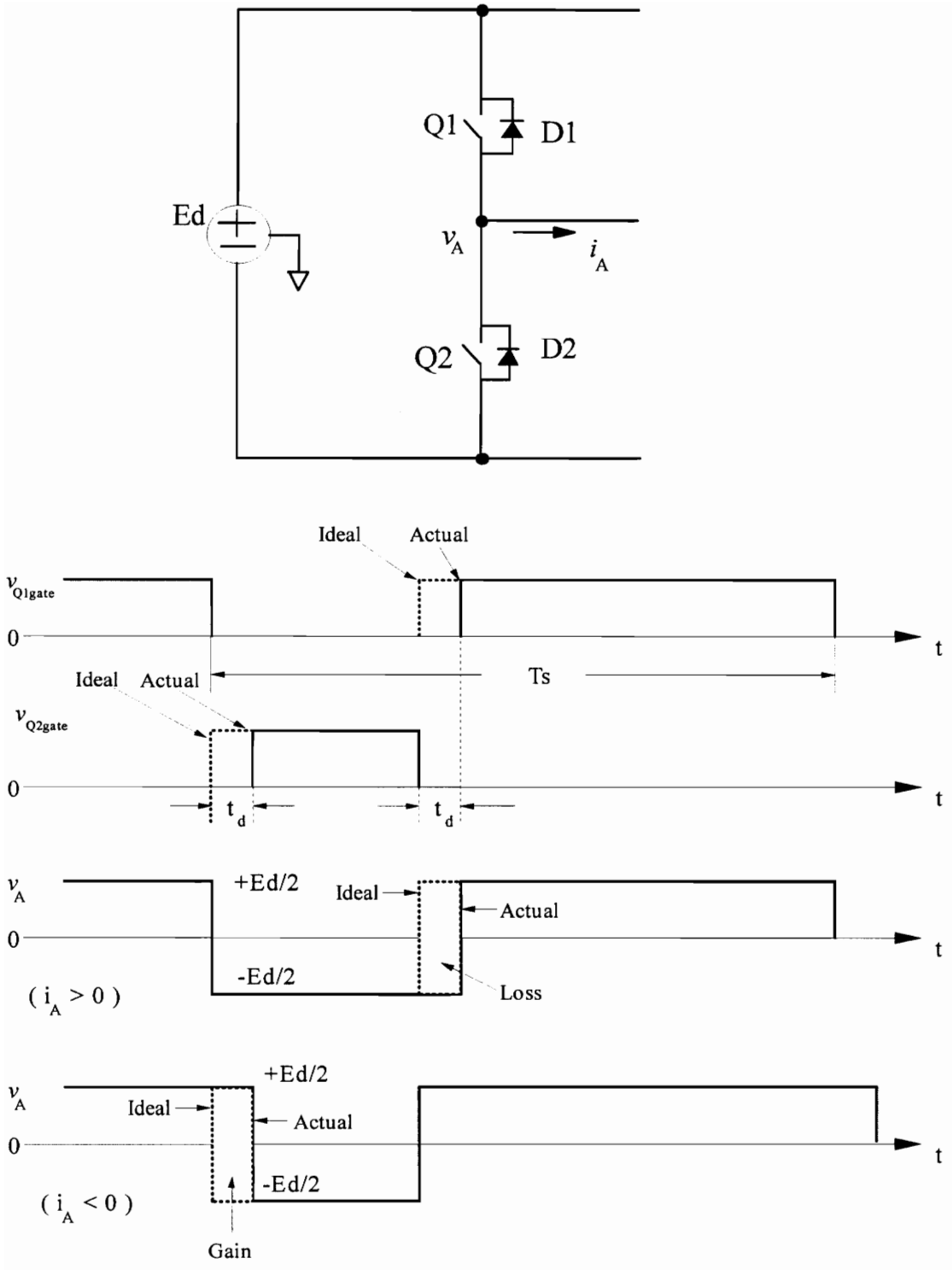

Fig. 2.7 Dead Time Effect on Output Voltage

Table 2.1

Percentage Reduction of Inverter Phase Output Voltage due to Dead Time Effect

$\Delta V/0.5E_d$	f_s = 10 KHz	f_s = 20 KHz	f_s = 30 KHz
t_d = 2 μs	4%	8%	12%
t_d = 3 μs	6%	12%	18%
t_d = 4 μs	8%	16%	24%

The direct effect of the dead time is a distortion of the waveform and a reduction in maximum inverter output voltage as shown in Figure 2.8 [3]. The effect on waveform distortion is out of the scope of the thesis. The effect of output voltage reduction is that the maximum motor speed is reduced. With regard to the inverter loss, the effect is insignificant. During the dead time, current conducts through diode instead of the IGBT on the other part of the same leg (i. e. instead of Q1, it is D2). Since the difference of the voltage drop of the IGBT and the diode is practically very small, and the dead time is normally short, the difference is practically negligible. But the maximum output voltage from the inverter is reduced as compared to ideal condition. This implied that the maximum achievable speed of a motor is reduced by the same percentage.

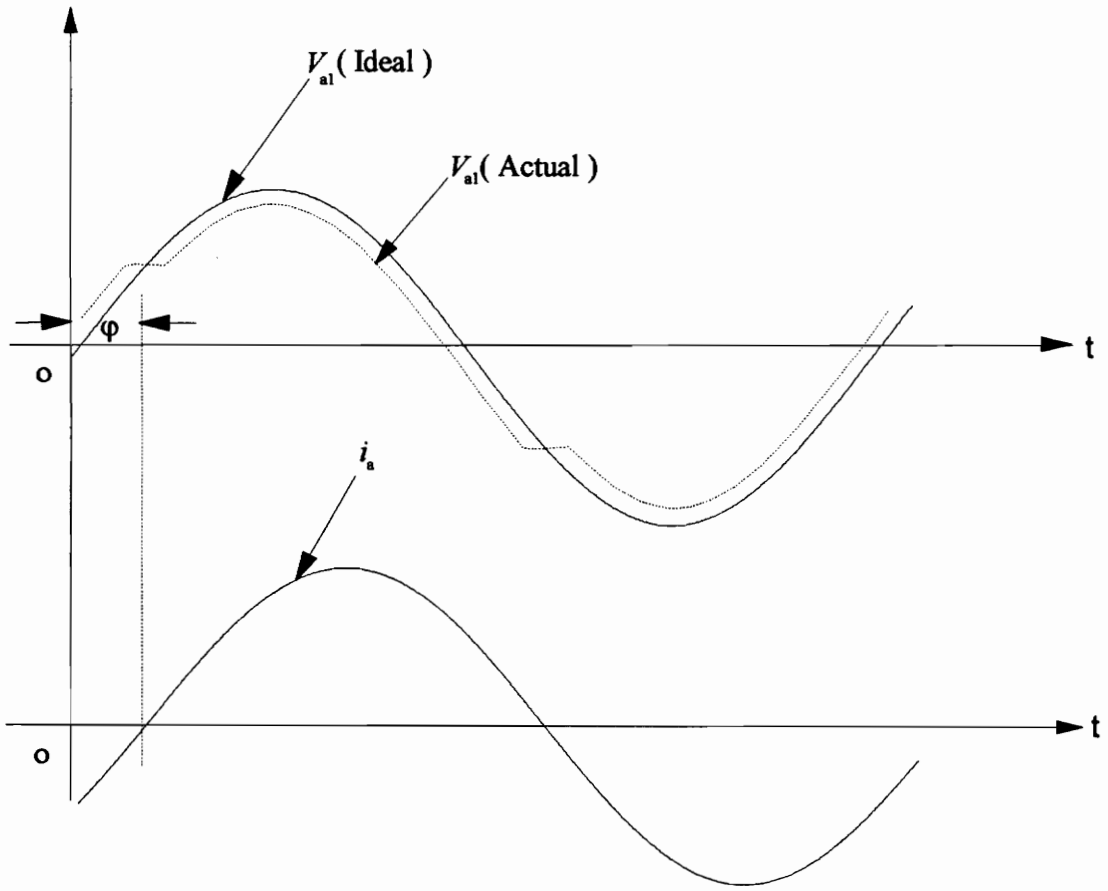

Fig. 2.8 Deat Time Effect on Fundamental Output Voltage

Chapter 3

Prediction of Inverter Losses and Device Junction Temperature Rise

Based on the description of inverter-motor operation given in Chapter 2, an algorithm will be developed to predict the inverter power losses and the junction temperature rise of power semiconductor devices used in the inverter. Equations for loss calculation will be described for both IGBTs and diodes for the three modes of motor operation: motoring, regeneration and stall. Using the loss calculation and the device thermal impedance information, the device temperature rise will be predicted.

3.1 Device Model for Loss Calculation

To find out the power losses in the power semiconductor devices, one needs to have loss models for the devices. Two loss mechanism are involved. One is conduction loss and the other is switching loss. Both are explained below.

3.1.1 Conduction loss model

To find out the device conduction loss, one needs to model the device static I - V characteristics. Fig. 3.1 shows the piece-wise linear characteristics of an IGBT or a diode.

$V_{CE} = V_{CE0} + R_Q \bullet I_{CE}$ for IGBT

$V_D = V_{D0} + R_D \bullet I_D$ for diode

To adequately model the static characteristics, V_{CE0} (or V_{D0}) and R_Q (or R_D) must be found. Both parameters can be obtained from manufacturer's data sheet.

3.1.2 Switching loss model

Switching losses include the turn-on loss, turn-off loss of both the IGBT and the diodes. This information is usually available from the manufacturer's data sheet nowadays. Figure 3.2 shows an example of such data. Notice that in Figure 3.2, the vertical axis is the energy lost per switching. Since most of the energy vs. current relationship are relatively linear, they are represented by equation as follows.

$EQ_{on} = h_1 \bullet i_c$

$EQ_{off} = h_2 \bullet i_c$

$ED_{rr} = h_3 \bullet i_d$

where, h_1, h_2 and h_3 are respective constant ratio which can be determined by setting an i_c value on the switching energy characteristics curves and dividing the i_c value into the corresponding switching energy losses value.

3.1.3 Temperature Effect on the Model

Temperature has impact effect on power losses of semiconductor devices. In general, IGBT conduction loss and switching loss increases with temperature. Diode conduction loss decreases but switching loss increases with temperature. The device parameters, therefore, changes with temperature. The changes of an example for temperature 25°C and 125°C are shown in Figure 3.2 and Figure 3.3. In order to predict the device power losses and junction temperature rise accurately, one need to know the device junction temperature based on which the device conduction and switching characteristics can be obtained. These characteristics on device junction temperature 25°C and 125°C are normally available from manufacturer's data sheet. Because the recommended maximum operating junction temperature is normally 125°C, the characteristics on temperature 125°C are used for the following device power losses calculations.

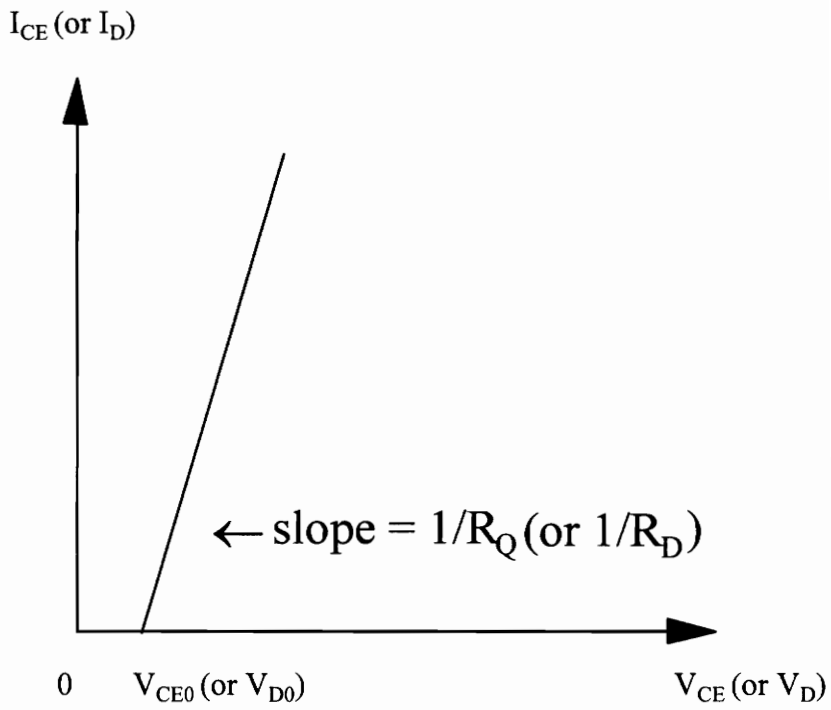

Fig. 3.1 Piece-Wise Characteristics of an IGBT or a Diode

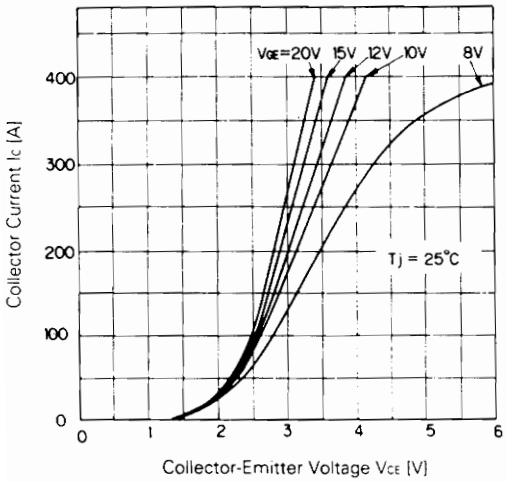

Collector Current vs. Collector-Emitter Voltage

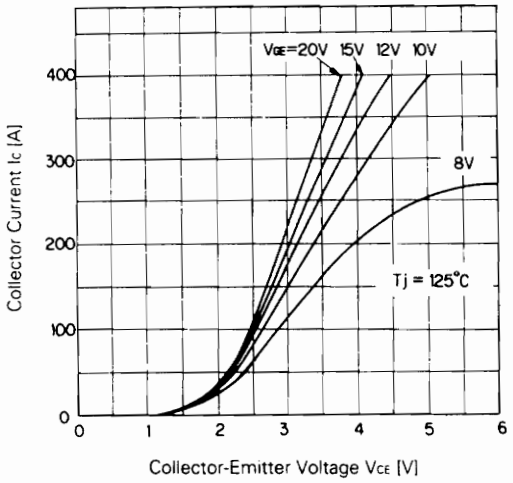

Collector Current vs. Collector-Emitter Voltage

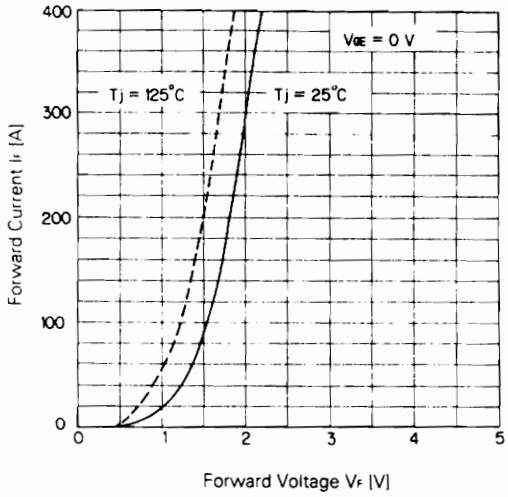

Forward Voltage of Free Wheel Diode

Fig. 3.2 An Example of Characteristics of IGBT and Diode

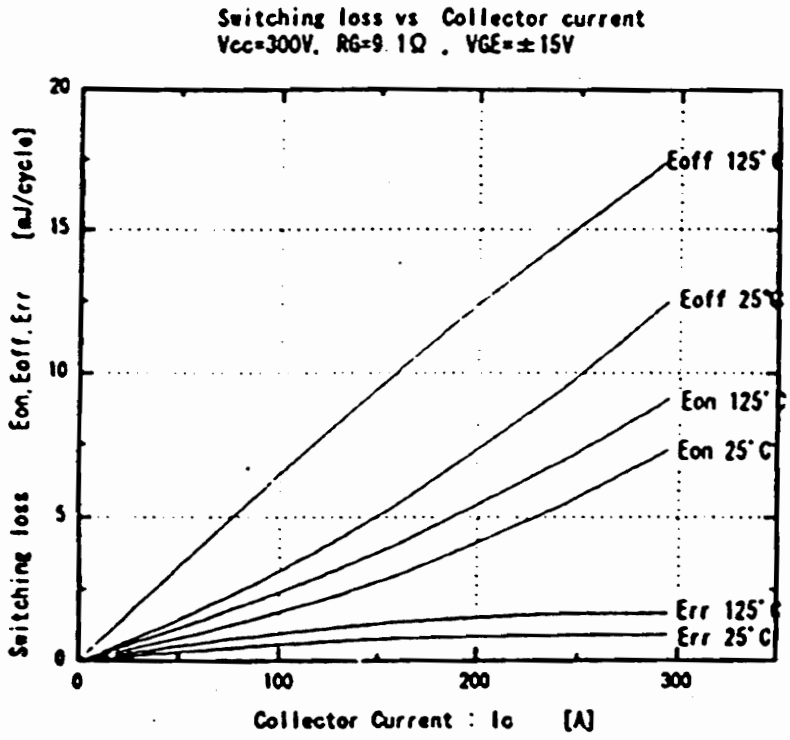

Fig. 3.3 Switching Losses Characteristcs

3.2 Inverter Loss Calculation

Equations for inverter loss calculation will be presented in this section for the three mode of motor operation: motoring, regeneration and stall. For all the three modes of operation, the first step to find out conduction loss is to determine the operating duty cycle of the switching devices. Because of PWM nature of the operation, the duty cycle of the IGBTs and diodes vary with time and motor operating condition.

3.2.1 Motoring Mode Loss Calculation

3.2.1.1 Determination of Duty Cycle

From a set of given motor parameters (R_s and L_s) and an operating condition (speed information is related to V_f and ω, torque information is related to I_a), one can find out V_{al} from Equations (2.2) and (2.3). The PWM modulation index m can then be obtained by $m = V_{al} / 0.5E_d$. Given these values, the duty cycle of IGBT and diode can be found by using Figure 3.4. In Figure 3.4, because the ratio of frequency between carrier signal V_t and reference voltage V_{ref} is high enough that V_{ref} can be considered as constant during a period of carrier signal, $a = V_{ref} (t = t_k) = mV_t\sin(\omega t_k + \varphi)$, $b = V_t$, where m is

modulation index, V_t is amplitude of the carrier signal, and $\frac{a+b}{b} = \frac{dTs}{\frac{1}{2}Ts}$. Therefore, the conduction duty cycle of the IGBTs dQ_m at $t = t_k$ can be represented as follows.

$$dQ_m(t_k) = \frac{d\,T_s}{T_s} = \frac{1}{2} \cdot \frac{a+b}{b} = \frac{1}{2}\left[1 + m\sin(\omega t_k + \varphi)\right]$$

Generally, $dQ_m = \frac{1}{2}\left[1 + m\sin(\omega t + \varphi)\right]$ for IGBT (3.1)

and the duty cycle for the opposing diode in the same phase (for example, Q1 vs. D2 or Q2 vs. D1) dD_m is expressed as follows.

$$dD_m = \frac{1}{2}\left[1 - m\sin(\omega t + \varphi)\right] \quad \text{for opposing diode in the same phase} \qquad (3.2)$$

It should be noted that in both equations shown above, the time reference is same as in Figure 2.2.

Figure 3.5 shows the duty cycle distribution of IGBTs and diodes in a leg of an inverter. When the motor is operated in a motoring mode, for given motor parameters (Rs, Ls, back-EMF constant K_b) and motor operating condition (speed and motor phase current), the conduction duty cycle dQm and dDm can be found by Equations (3.1) and (3.2).

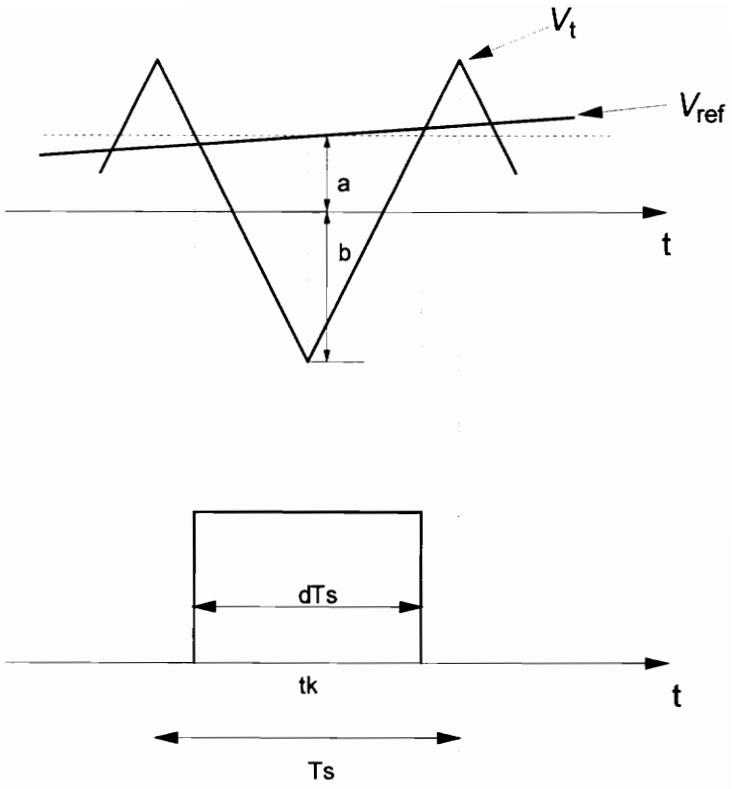

Fig. 3.4 Sinusoidal PWM Waveform Generating

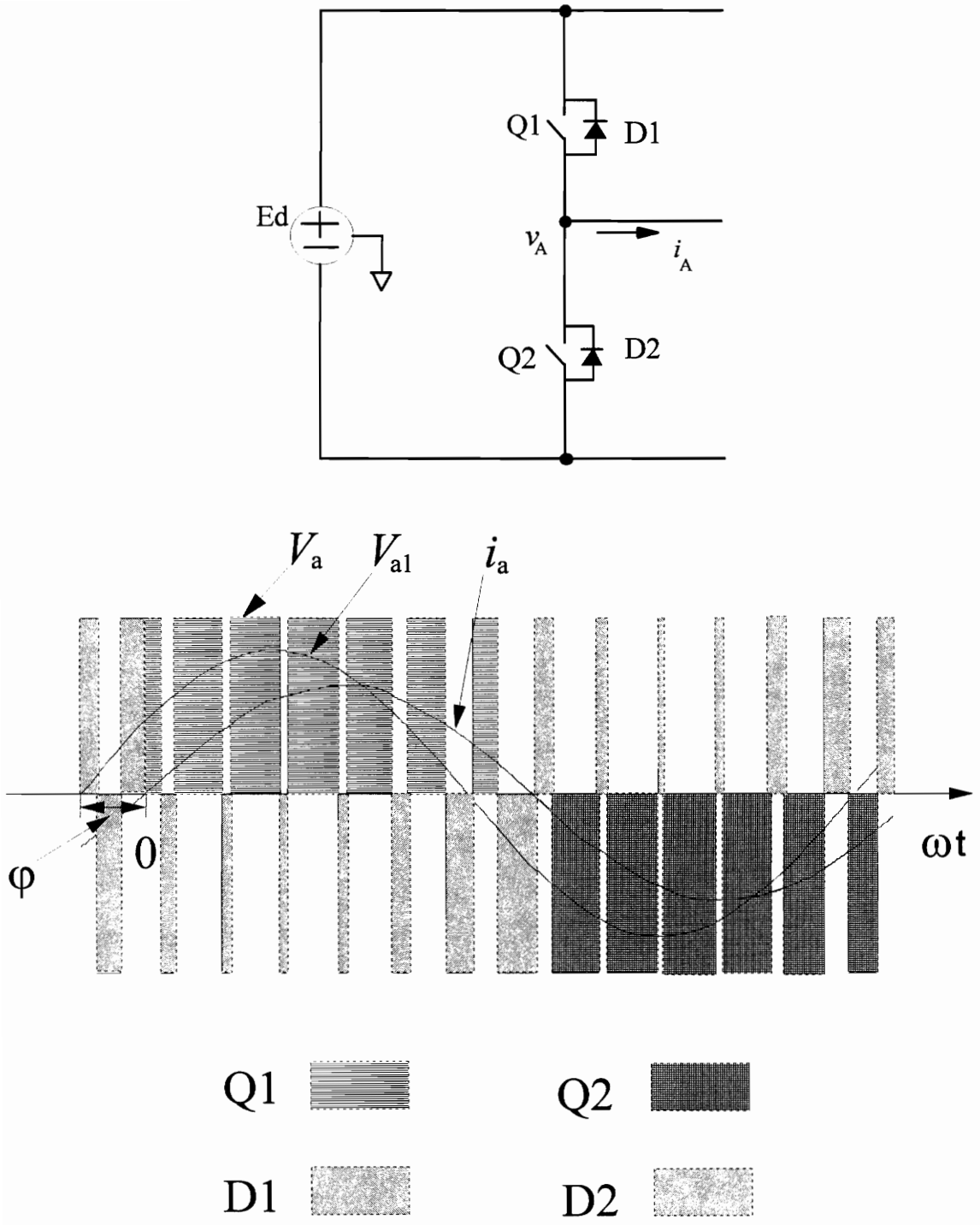

Fig. 3.5 Conduction Distribution of IGBTs and Diodes for Motoring Mode Operation

3.2.1.2 Loss Calculation

A. Conduction Loss

The harmonic distortion of the inverter output current waveform is normally low since most of the time the ratio between the carrier (PWM switching) frequency is high. For this reason, a pure sinusoidal current waveform of the inverter is assumed for power losses calculation in this chapter. Therefore the average conduction loss for each high-frequency PWM cycle can be expressed PQ_c for IGBT loss and PD_c for diode loss as follows

$$PQ_c(\omega t) = i_{ce}(\omega t)V_{CE}(\omega t)dQ_m(\omega t)$$

$$= I_{pk}\sin\omega t(V_{CE0} + R_Q I_{pk}\sin\omega t)0.5[1+m\sin(\omega t +\varphi)] \quad \text{for IGBTs} \quad (3.3)$$

$$PD_c(\omega t) = i_d(\omega t)V_D(\omega t)dD_m(\omega t)$$

$$= I_{pk}\sin\omega t(V_{D0} + R_D I_{pk}\sin\omega t)\ 0.5[1-m\sin(\omega t +\varphi)] \quad \text{for diodes} \quad (3.4)$$

Notice that both expressions are function of time. By integrating the above high-frequency average power loss over one low-frequency (fundamental) current period, the average conduction power losses are as follows

$$PQm_c = \frac{R_Q I_{pk}^2}{4\pi}\left(\frac{\pi}{2} + \frac{4}{3}m\cos\varphi\right) + \frac{V_{Q0} I_{pk}}{2}\left(\frac{1}{\pi} + \frac{m}{4}\cos\varphi\right) \quad (3.5)$$

$$PDm_c = \frac{R_D I_{pk}^2}{4\pi}\left(\frac{\pi}{2} - \frac{4}{3}m\cos\varphi\right) + \frac{V_{D0} I_{pk}}{2}\left(\frac{1}{\pi} - \frac{m}{4}\cos\varphi\right) \quad (3.6)$$

From Equations. (3.3) and (3.4), it can be seen that the device conduction loss depends on device parameters (V_{Q0}, V_{D0}, R_Q and R_D), modulation index m, phase angle φ between the phase voltage and phase current, and the peak of the phase current.

B. Switching Losses

The switching energy data of a device are usually given by the manufacturers for a fixed bus voltage and gate drive condition (See Figure 3.2). Since the switching energy is practically proportional to the actual bus voltage E_d and varies with actual gate drive, for application purpose, the above switching energy equations need to be scaled for the operating voltage and for actual gate drive. The scaled equations are as follows

$$EQ_{on} = k_{gon} \bullet (E_d / V_{test}) \bullet h_1 \bullet i(\omega t) \quad (3.7)$$

$$EQ_{off} = k_{goff} \bullet (E_d / V_{test}) \bullet h_2 \bullet i(\omega t) \quad (3.8)$$

$$ED_{rr} = k_{grr} \bullet (E_d / V_{test}) \bullet h_3 \bullet i(\omega t) \quad (3.9)$$

where k_{gon}, k_{goff} and k_{grr} are the constants normally determined by gate drive resister value used, which affects device switching speed. In the thesis, k_{gon}, k_{goff} and k_{grr} are all set to be unity for the discussion. The instantaneous power loss in one IGBT or one diode at any time during one cycle of the carrier frequency is obtained by multiplying switching energy by the carrier frequency. The average switching power loss is obtained by integrating the instantaneous loss over the fundament frequency. The results are as follows

$$PQm_{on} = \frac{1}{2\pi}\int_0^{\pi} f_s \cdot \frac{V_{bus}}{V_{test}} \cdot h_1 \cdot I_{pk} \sin\omega t d(\omega t)$$

$$= f_s \bullet (E_d/V_{test}) \bullet h_1 \bullet I_{pk}/\pi \qquad (3.10)$$

$$PQm_{off} = \frac{1}{2\pi}\int_0^{\pi} f_s \cdot \frac{V_{bus}}{V_{test}} \cdot h_2 \cdot I_{pk} \sin\omega t d(\omega t)$$

$$= f_s \bullet (E_d/V_{test}) \bullet h_2 \bullet I_{pk}/\pi \qquad (3.11)$$

$$PDm_{rr} = \frac{1}{2\pi}\int_0^{\pi} f_s \cdot \frac{V_{bus}}{V_{test}} \cdot h_3 \cdot I_{pk} \sin\omega t d(\omega t)$$

$$= f_s \bullet (E_d/V_{test}) \bullet h_3 \bullet I_{pk}/\pi \qquad (3.12)$$

C. Total Power Losses

The equation for calculating the various losses are summarized as follows:

The total power loss for each IGBT PQm_{total} consists of conduction loss PQm_c, the turn-on loss PQm_{on} and the turn-off loss PQm_{off}.

$$PQm_{total} = PQm_c + PQm_{on} + PQm_{off}$$

$$= \frac{R_Q I_{pk}^2}{4\pi}\left(\frac{\pi}{2} + \frac{4}{3}m\cos\varphi\right) + \frac{V_{Q0} I_{pk}}{2}\left(\frac{1}{\pi} + \frac{m}{4}\cos\varphi\right)$$

$$+ f_s \bullet (E_d/V_{test}) \bullet h_1 \bullet I_{pk}/\pi$$

$$+ f_s \bullet (E_d/V_{test}) \bullet h_2 \bullet I_{pk}/\pi \qquad \text{for each IGBT} \qquad (3.13)$$

By the same token, the total power loss for each diode is

$$PDm_{total} = PDm_c + PDm_{rr}$$

$$= \frac{R_D I_{pk}^2}{4\pi}\left(\frac{\pi}{2} - \frac{4}{3}m\cos\varphi\right) + \frac{V_{D0} I_{pk}}{2}\left(\frac{1}{\pi} - \frac{m}{4}\cos\varphi\right)$$

$$+ f_s \bullet (E_d/V_{test}) \bullet h_3 \bullet I_{pk}/\pi \qquad \text{for each diode} \qquad (3.14)$$

Since there are totally six pairs of IGBT and diode in an inverter, the total inverter power losses are as follows.

$$Pm_{total} = 6 \times (PQm_{total} + PDm_{total}) \qquad (3.15)$$

The right-hand side of the Equations (3.13), (3.14) and (3.15) consists of several sets of parameters as discussed in the following:

Power semiconductor device parameters R_Q, R_D, V_{Q0}, V_{D0}: All can be found out from manufacturers data sheet.

Amplitude of phase current I_{pk}: This value can be found out if the torque output is given and the motor torque constant is known. Torque = $K_t \times I_{pk}$, K_t is motor torque constant.

Modulation index m: It can be derived from Equation (2.3) if the inverter bus voltage the motor parameters, the motor speed and the phase current are known.

Phase angle φ: It can be found out from Equation (2.2), if the motor parameters, the motor speed and the phase current are known.

Therefore, for a given set of device and motor parameter value and operating condition, the loss can be found.

3.2.2 Regenerating Mode Loss Calculation

3.2.2.1 Determination of Duty Cycle

Referring to Figure 2.4 and Figure 3.6, due to the reversal polarity of V_{ref} in this mode, the phase current $\mathbf{I_a}$ is 180° out of phase with $\mathbf{V_f}$ and therefore nearly 180° out of phase with V_{ref} or V_{a1}. With i_a as reference, i.e. $i_a = I_{pk}\sin\omega t$, then $V_{a1} = -m\frac{E_d}{2}\sin(\omega t - \varphi)$.

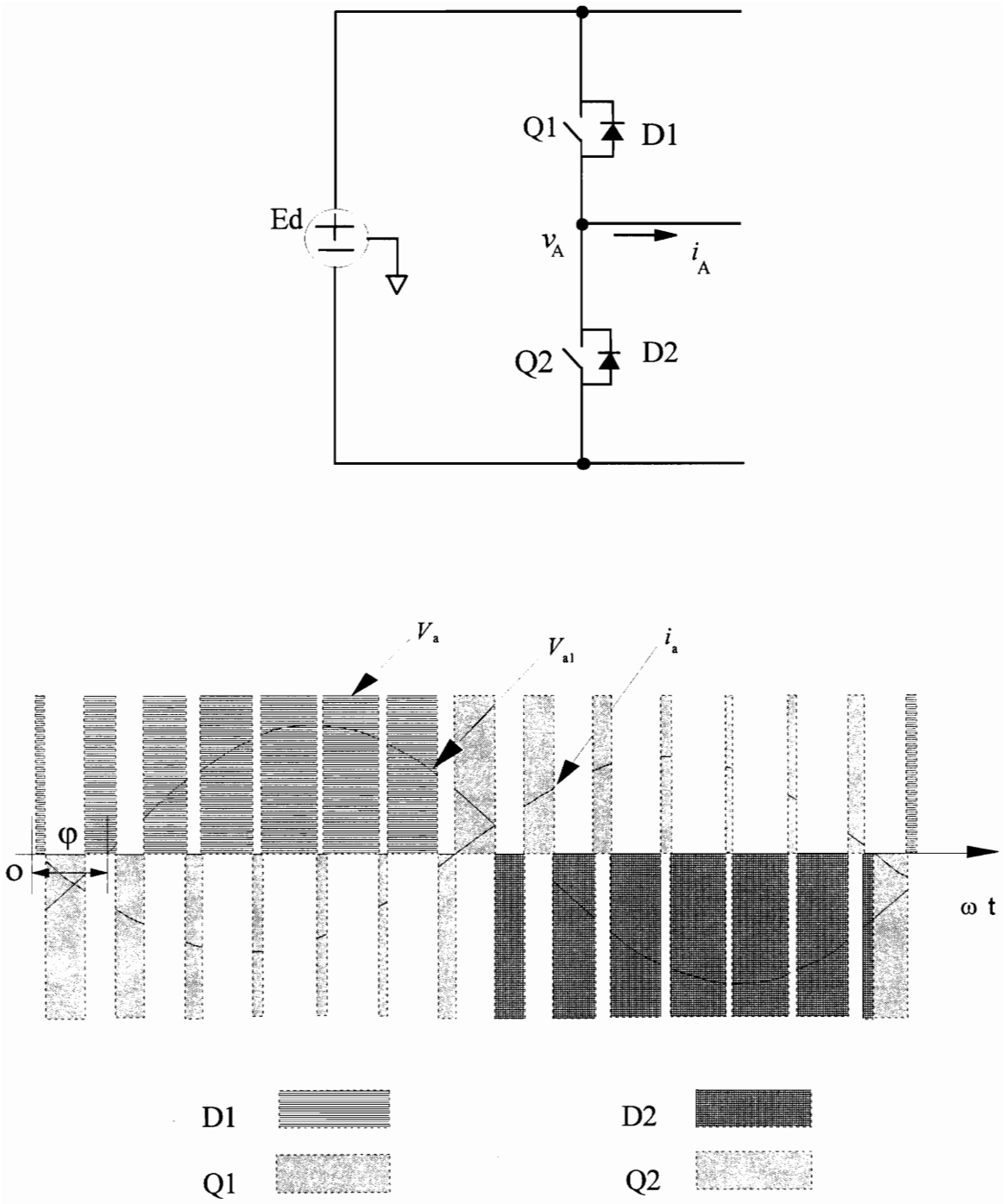

Fig. 3.6 Conduction Distribution of IGBTs and Diodes for Regen. Mode Operation

$$dQ_r = \frac{1}{2}[1 - m\sin(\omega t - \varphi)] \quad \text{for IGBTs} \qquad (3.16)$$

$$dD_r = \frac{1}{2}[1 + m\sin(\omega t - \varphi)] \quad \text{for diodes} \qquad (3.17)$$

Notice that expression(3.16) for IGBTs is similar to (3.2) for diodes in motoring mode and (3.17) similar to (3.1) for IGBTs in motoring mode, which means that diodes conduct longer time than IGBTs in this mode of operation. Figure 3.6 shows the conduction distribution of IGBT and diode in this mode.

3.2.2.2 Loss Calculation

A. Conduction Loss

In the regenerating mode, because current feed back is positive during the regenerating interval, the phase current is driven as high as up to the current limit of the inverter. As large load inertia assumption made before, the worst condition in which the rectifier runs the current with the current limit level is assumed due to the current decaying very slowly for the following losses calculations. Therefore, the average conduction loss for each high-frequency cycle can be expressed as follows

$$PQ_{rc}(\omega t) = i_{ce}(\omega t) \bullet V_{CE}(\omega t) \bullet dQ_r(\omega t)$$

$$= I_m \sin\omega t \bullet (V_{CE0} + R_Q \bullet I_m \sin\omega t) \bullet 0.5(1 - m\sin(\omega t - \varphi)) \quad \text{for IGBTs} \qquad (3.18)$$

$$PD_{rc}(\omega t) = i_d(\omega t) \bullet V_D(\omega t) \bullet dD_m(\omega t)$$

$$= I_{pk}\sin\omega t \bullet (V_{D0} + R_D \bullet I_m \sin\omega t) \bullet 0.5(1+m\sin(\omega t - \varphi)) \text{ for diodes} \quad (3.19)$$

By integrating the above high-frequency average power loss over one low-frequency (fundamental) current period, the average conduction power losses are as follows

$$PQr_c = \frac{R_Q I_m^2}{4\pi}\left(\frac{\pi}{2} - \frac{4}{3}m\cos\varphi\right) + \frac{V_{Q0} I_m}{2}\left(\frac{1}{\pi} - \frac{m}{4}\cos\varphi\right) \quad (3.20)$$

$$PDr_c = \frac{R_D I_m^2}{4\pi}\left(\frac{\pi}{2} + \frac{4}{3}m\cos\varphi\right) + \frac{V_{D0} I_m}{2}\left(\frac{1}{\pi} + \frac{m}{4}\cos\varphi\right) \quad (3.21)$$

B. Switching Loss

The average switching power loss are as follows

$PQr_{on} = f_s \bullet (E_d/V_{test}) \bullet h_1 \bullet I_m/\pi$

$PQr_{off} = f_s \bullet (E_d/V_{test}) \bullet h_2 \bullet I_m/\pi$

$PDr_{rr} = f_s \bullet (E_d/V_{test}) \bullet h_3 \bullet I_m/\pi$

C. Total Power Losses

$PQr_{total} = PQr_c + PQr_{on} + PQr_{off}$ for IGBT

$PDr_{total} = PDr_c + PDr_{rr}$ for diode

$Pr_{total} = 6\times(PQr_{total} + PDr_{total})$ for inverter

3.2.3 Stalled Mode Loss Calculation

3.2.3.1 Determination of Duty Cycle

As in the case of motoring mode operation, the first step to find out losses under stalled condition is to find the duty cycle information under this condition. An example of the inverter operating under this condition is shown in Figure 3.7. Notice that no back-EMF is present because the motor is at stall. From the Kirchhoff voltage law, the following equations are obtained:

$$V_{ao} - V_{bo} = (I_a + I_b)R_s$$

$$V_{ao} - V_{co} = (I_a + I_c)R_s$$

$$V_{ao} + V_{bo} + V_{co} = 0$$

where V_{ao}, V_{bo} and V_{co} are average voltage, R_s is the phase winding resistance.

Solve above equations and notice that $I_a = I_b + I_c$, then

$$dQ_1 = \frac{1}{2} + \frac{R_s}{3E_d}(2I_a + I_b + I_c) = \frac{1}{2} + \frac{R_s}{E_d}I_a$$

$$dD_2 = \frac{1}{2} - \frac{R_s}{3E_d}(2I_a + I_b + I_c) = \frac{1}{2} - \frac{R_s}{E_d}I_a$$

$$dD_3 = \frac{1}{2} - \frac{R_s}{3E_d}(I_a + 2I_b - I_c) = \frac{1}{2} - \frac{R_s}{E_d} I_b$$

$$dQ_4 = \frac{1}{2} + \frac{R_s}{3E_d}(I_a + 2I_b - I_c) = \frac{1}{2} + \frac{R_s}{E_d} I_b$$

$$dD_5 = \frac{1}{2} - \frac{R_s}{3E_d}(I_a - I_b + 2I_c) = \frac{1}{2} - \frac{R_s}{E_d} I_c$$

$$dQ_6 = \frac{1}{2} + \frac{R_s}{3E_d}(I_a - I_b + 2I_c) = \frac{1}{2} + \frac{R_s}{E_d} I_c$$

Summarily, $dQ_s = 0.5 + I_{dc} \bullet R_s/E_d$ (3.22)

$dD_s = 0.5 - I_{dc} \bullet R_s/E_d$ (3.23)

where I_{dc} is the DC current flowing through one phase of the motor. If $I_{dc} \bullet R_s << E_d$, (in most applications it is true), $dQ_s = dD_s = 0.5$

From above discussion, it can be seen that at stalled condition, the diode conducts nearly 50% while the IGBT takes slightly above 50% current. Compared to the motoring-mode operation, the diode takes more average current.

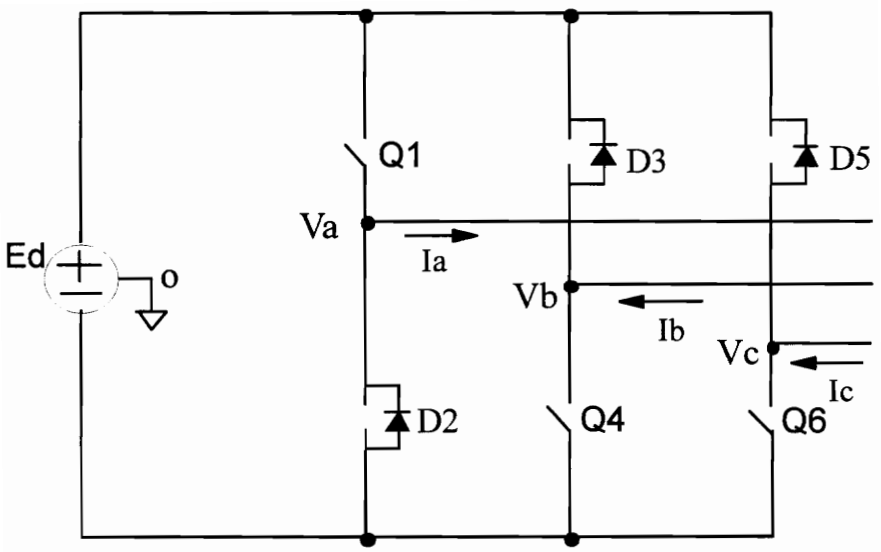

Fig. 3.7 Circuit of Stalled Mode Operation

3.2.3.2 Loss Calculation

A. Conduction Loss

The conduction losses of one IGBT and its corresponding diode are represented by

$PQs_c = V_{CE} \bullet I_{dc} \bullet dQ_s$ for IGBTs

$PDs_c = V_D \bullet I_{dc} \bullet dD_s$ for diodes

B. Switching Loss

In the stalled operation, one IGBT and its corresponding diode commutate with the DC current for each PWM switching. Therefore, the switching loss of the IGBT and the reverse recovery loss of the diode are simply as follows

$PQs_{on} = f_s \bullet (E_d/V_{test}) \bullet h_1 \bullet I_{dc}$ for IGBT turn-on loss

$PQs_{off} = f_s \bullet (E_d/V_{test}) \bullet h_2 \bullet I_{dc}$ for IGBT turn-off loss

$PDs_{rr} = f_s \bullet (E_d/V_{test}) \bullet h_3 \bullet I_{dc}$ for diode reverse recovery loss

C. Total Power Losses

$PQs_{total}(n) = PQs_c(n) + PQs_{on}(n) + PQs_{off}(n)$ for IGBT (n = 1, 2, 3)

$PDs_{total}(n) = PDs_c(n) + PDs_{rr}(n)$ for diode (n = 1, 2, 3)

$Ps_{total} = \sum_{n=1}^{3} [\, PQs_{total}(n) + PDs_{total}(n) \,]$ for inverter

3.3 Junction Temperature Rise of Devices

The junction temperature of a power semiconductor device is a major concern for an inverter design, which is determined by the device power losses, ambient temperature around it and the heat conduction condition.

3.3.1 Thermal Equivalent Circuit

The heat transfer path can be expressed as an equivalent electrical circuit as shown in Figure 3.8, where P is the power dissipation, T_j is device junction temperature, T_c is device case temperature, T_f is heat sink fin temperature and R_{th} is thermal resistance. Due to $R_{th(c-a)}$ is considerable larger than the others of a device, the total thermal resistance $R_{th(j-a)}$ from the junction to the atmosphere can be expressed as follows.

$$R_{th(j-a)} = R_{th(j-c)} + R_{th(c-f)} + R_{th(f-a)} \qquad (3.24)$$

In the case that a pulse power waveform is short in duration, transient thermal impedance r_{th} of a device should be used due to thermal capacity besides thermal resistance. Figure 3.9 shows an example of a typical device junction to case normalized transient thermal impedance characteristics for a 600-V, 200-A IGBT module, which is a

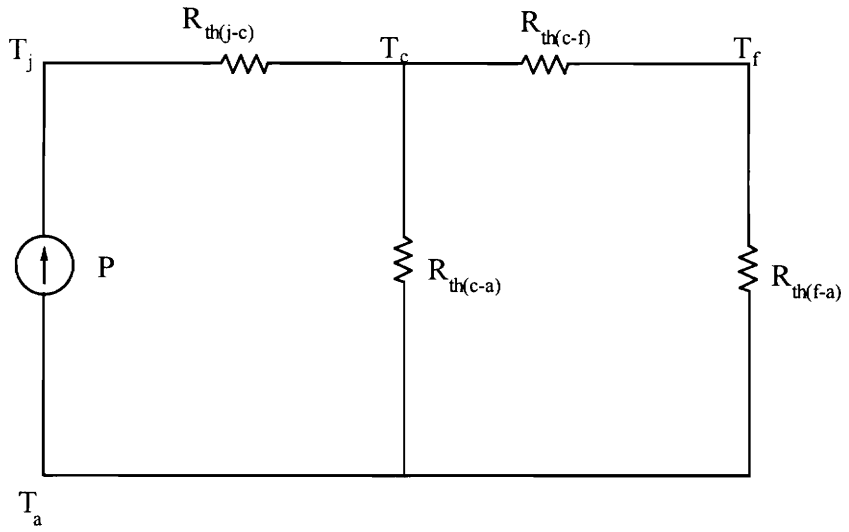

$R_{th(j-a)}$: Device junction to ambient steady state thermal resistamce

$R_{th(j-c)}$: Device junction to case steady state thermal resistance

$R_{th(c-f)}$: Device case to heatsink fin steady state thermal resistance

$R_{th(f-a)}$: Device heatsink fin to ambient steady state thermal resistance

Fig. 3.8 Device Thermal Equivalent Circuit

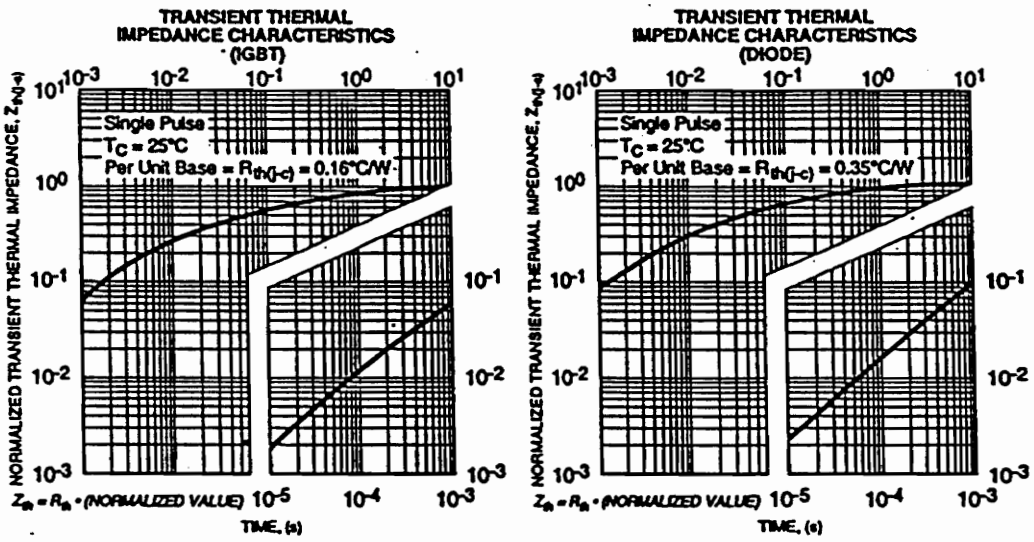

Fig. 3.9 An Example of Transient Thermal Impedance Characteristics

ratio of the real transient thermal resistance to the steady state thermal resistance (i.e. r = r_{th}/R_{th}, where r is the normalized thermal resistance, rth is the transient thermal resistance and Rth is the steady state thermal resistance). It can be seen that the transient thermal resistance for this particular device that when the power pulse duration is less than 2 second, the transient thermal impedance is smaller than a steady-state thermal impedance. For example, if the power pulse is 5 millisecond, then the normalized thermal resistance r for IGBT is 0.2 and the real transient thermal resistance $r_{th}(5\ ms) = r \times R_{th} = 0.2 \times 0.16 =$ 0.032 °C/W, where $R_{th} = 0.16$ °C/W.

3.3.2 Calculation of Device Temperature Rise

For a constant power dissipation, the device junction temperature rise can be simply expressed as follows

$$T_j - T_a = P_0 \times R_{th(j-a)}\ , \text{or} \qquad (3.25)$$

$$T_j - T_c = P_0 \times R_{th(j-c)} \qquad (3.26)$$

Where, $R_{th(j-a)}$ or $R_{th(j-c)}$ is steady state thermal resistance between junction and ambient and between junction and case respectively.

For the pulse power condition as shown in Figure 3.10, the junction temperature can be determined from the delayed power step pulse and power superimposition principle using Equations (3.27) and (3.28) as follows[8].

$$\Delta T_{j1} = P_1 \times r_{th}(t_1) \qquad (3.27)$$

$$\Delta T_{j2} = P_1 \times [\, r_{th}(t_3) - r_{th}(t_3 - t_1) \,] + P_2 \times r_{th}(t_3 - t_2) \qquad (3.28)$$

Where, r_{th} is a transient thermal resistance, $\Delta T_{j1} = T_{j1} - T_a$ at $t = t_1$, $\Delta T_{j2} = T_{j1} - T_a$ at $t = t_2$ (T_a is ambient temperature).

By using a two pulse approximation, the junction temperature rise for a long power pulse train can be expressed by Equation (3.29) as follows[8].

$$T_j = P_{AVE} \times R_{th} + (P - P_{AVE}) \times r_{th}(T + \tau) - P \times r_{th}(T) + P \times r_{th}(\tau) + T_c \qquad (3.29)$$

R_{th}: Device steady state thermal resistance

$r_{th}(\tau)$: Device transient thermal resistance for power pulse of τ duration

τ: Power pulse width

P: Power pulse peak value

P_{AVE}: Power pulse average value for a period T

T: Power Pulse Period

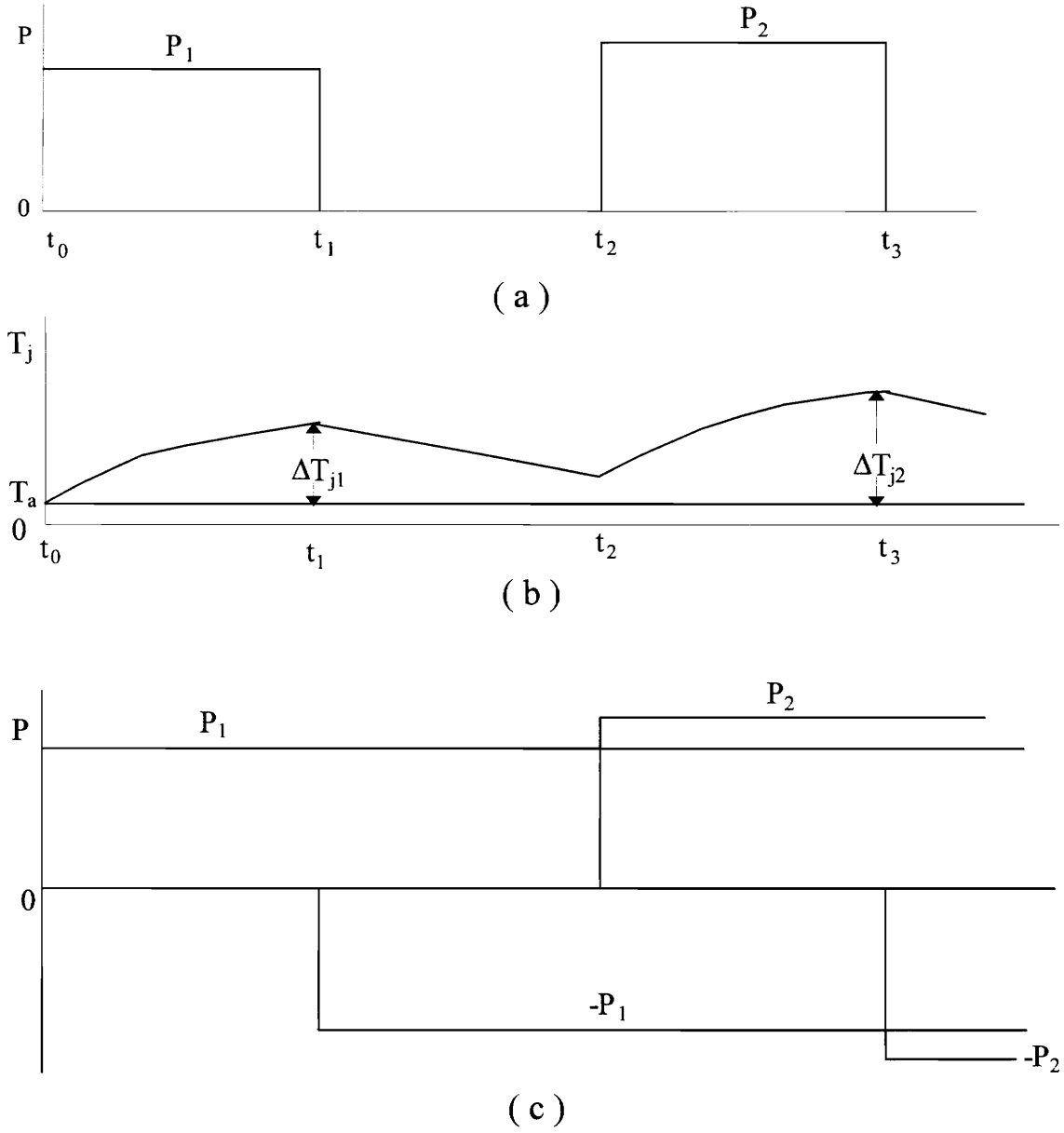

Fig. 3.10 (a) Pulse Power Dissipation Waveform
(b) Junction Temperature
(c) Step Waveform Superimposition

3.3.3 Device Instantaneous Power Dissipation

From Figure 3.4 and Equation (3.3), (3.4) (3.7) (3.8) and (3.9), it can be seen that the instantaneous power dissipation in a device is a function of time as shown in Figure 3.11 where the frequency of the fundamental phase current is f_0. Because the PWM frequency is normally large enough that the device temperature fluctuation between high frequency PWM pulses is negligible. Therefore average power dissipation (average over high frequency PWM cycle) is used for the discussion of device temperature calculation. For the convenience of predicting device junction temperature rise, an approximated power dissipation waveform P_0 is used, where the area of the rectified sinusoidal power dissipation waveform is the same as the area of the rectangular P_0 waveform. Therefore, the approximated power dissipation waveform P_0 will be used for the calculation of device temperature information as discussed in the following section.

.

3.3.4 Prediction of Temperature Rise for Inverter Power Semiconductor Devices

Defining f_0 as the fundamental current frequency, $T_0 = 1/f_0$, τ the device power dissipation pulse width as shown in Figure 3.11 and t_τ a time point at which the device ransient resistance reaches the steady state value (for example, in Figure 3.9, $t_\tau = 1s$),

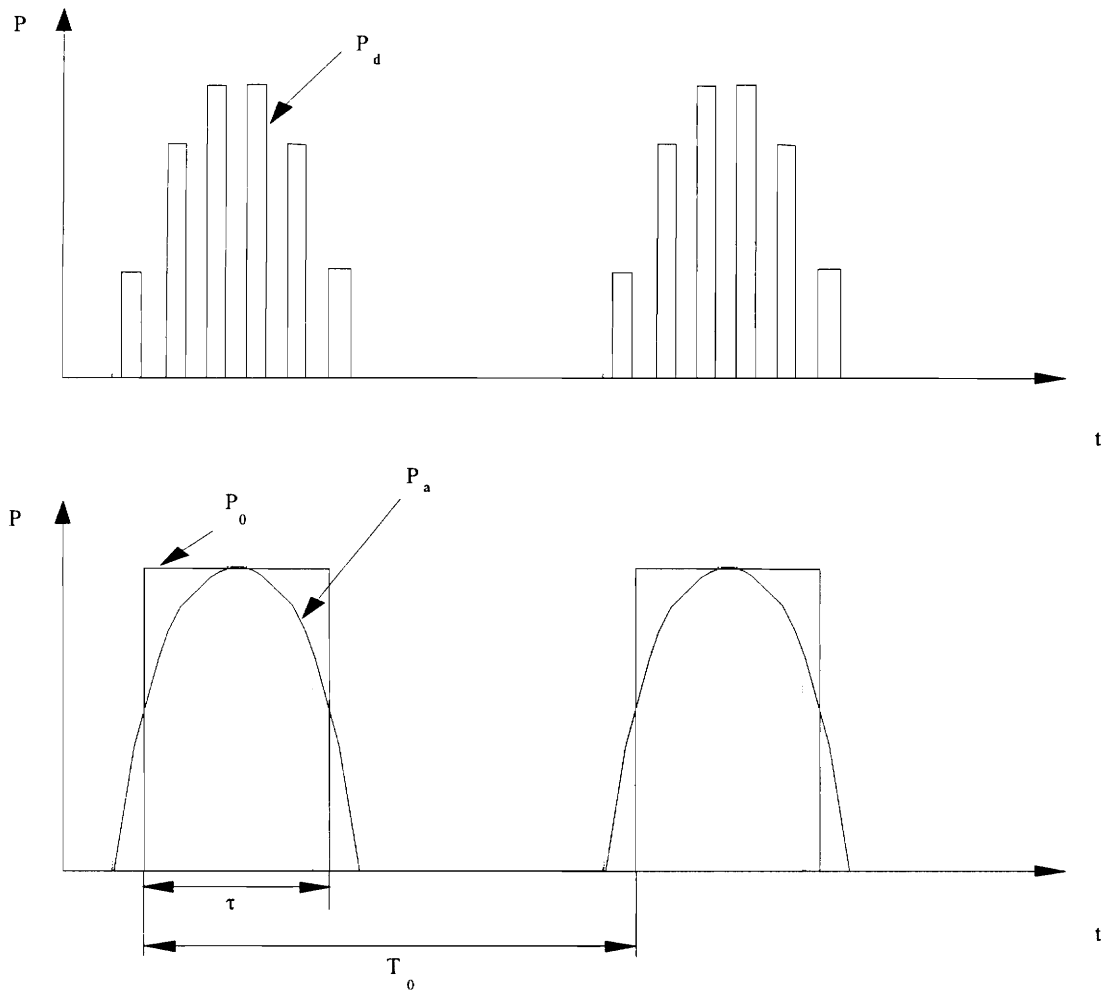

P_d : Instantaneous Power Dissipation

P_a : Average Power Dissipation over PWM Frequency

P_0 : Approximated Power Dissipation

Fig. 3.11 Device Instantaneous Power Waveform

two different conditions are classified for the calculation of device junction temperature rise, depending on relatively comparison of the power dissipation pulse width τ, the fundamental period T_0 and t_τ.

Case (A): $\tau < T_0 < t_\tau$

When τ and T_0 are less than t_τ, Equation (3.29) is used to predict the device junction temperature rise.

Case (B): $t_\tau \leq \tau < T_0$

τ is larger than t_τ, all transient thermal resistance in Equation (3.29) are equal to the steady state thermal resistance. i. e. $r_{th}(T + \tau) = r_{th}(T) = r_{th}(\tau) = R_{th}$).

Therefore

$$T_j = P_{AVE} \times R_{th} + (P - P_{AVE}) \times r_{th}(T + \tau) - P \times r_{th}(T) + P \times r_{th}(\tau) + T_c$$

$$= P_{AVE} \times R_{th} + (P - P_{AVE}) \times R_{th} - P \times R_{th} + P \times R_{th} + T_c$$

$$= P \times R_{th} + T_c \qquad (3.30)$$

Notice that $P = P_0$ in Equation (3.30).

When the motor is running very slowly (i.e. T_0 very long), Case (B) Equation should be used. Since P_0 is always greater than P_{AVE}, the device temperature rise is worst for case (B), which is the same as the worst condition in stalled mode.

Assume that the device power dissipation pulse width $\tau \approx \frac{T_0}{2}$, N is motor speed (RPM), α is the number of poles of a motor. Since $N = \frac{120 f_0}{\alpha} = \frac{120}{\alpha \cdot T_0}$, and according to discussions above, when $\tau \approx \frac{T_0}{2} \geq t_\tau$, i.e. $T_0 \geq 2t_\tau$ ($N \leq \frac{60}{\alpha \cdot t_\tau}$), Case (B) should be used. This means that the device temperature rise in the case, when the motor RPM is low, could be severe.

3.4 Flow Chart for Predicting Power Losses and Device Temperature Rise

Using the equations for calculating losses described in section 3.2 and the equations for calculating device temperature rise, a flow chat for predicting the inverter power losses and the devices junction temperature rise is shown in Figure 3.12. An example of the program inputs and outputs for junction temperature 25°C and 125°C is shown in the following:

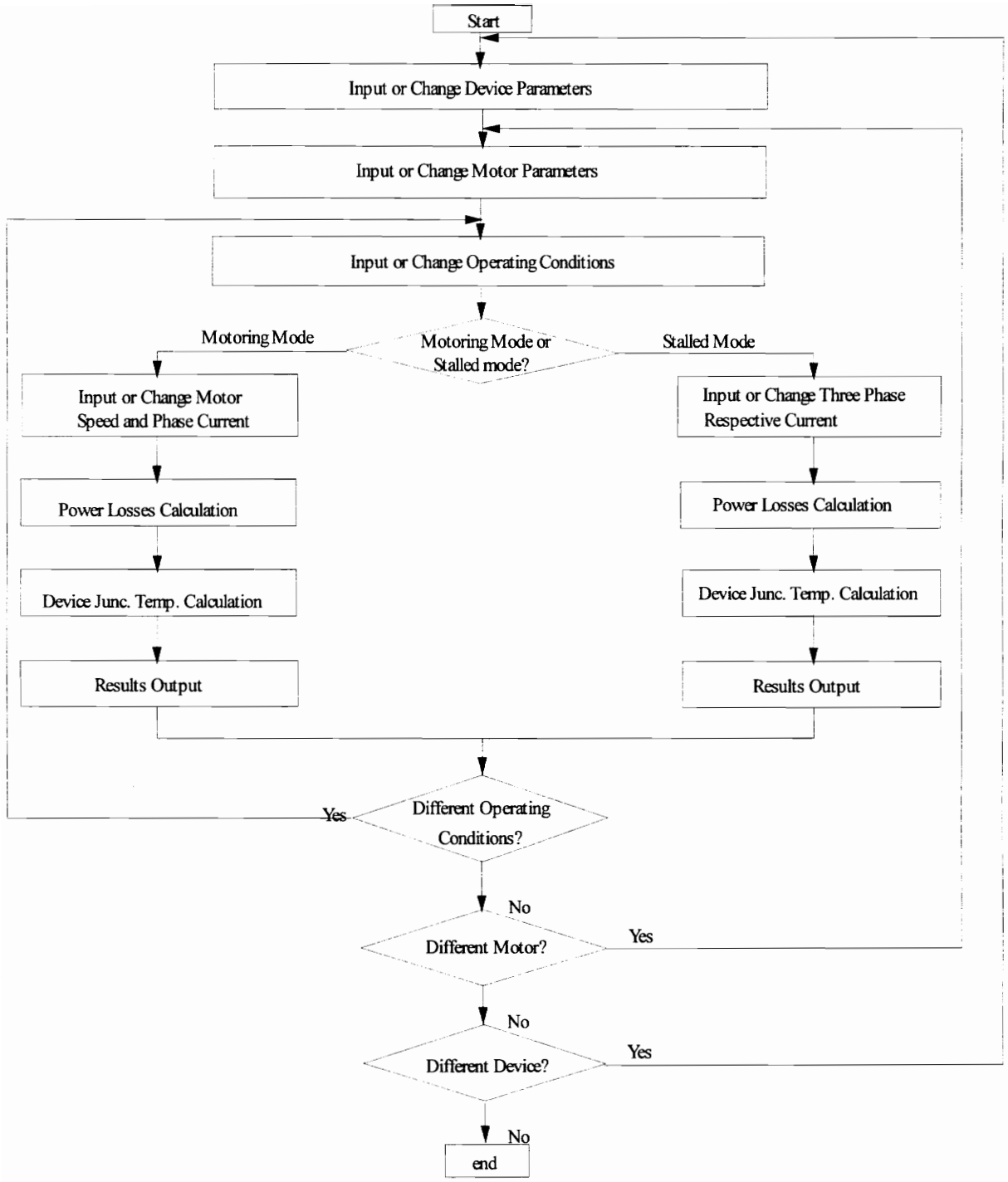

Fig. 3.12 Flow Chart of the Computer Program

Junction Temperature = 25°C:

Input of Program:

1 - Power device part #: 2MBI150L - 120 (Fuji's 150 A 1200 V L Series IGBT)

2 - Motor #: B36 -152 - EBA - 26 (Motion Control Systems, Inc.)

3 - IGBT minimum V_{q0}: 2 (V)

4 - Device characteristics testing current I_{test}: 150 (A)

5 - IGBT voltage at the testing current V_q: 2.75 (V)

6 - Diode minimum V_{d0}: 1.25 (V)

7 - Diode forward voltage at the testing current V_d: 1.8 (V)

8 - IGBT turn - on switching loss E_{on} at I_{test}: 21 (mJ)

9 - IGBT turn - off switching loss E_{off} at I_{test}: 16.62 (mJ)

10 - Diode reverse recovery loss E_{rr} at I_{test}: 5.2 (mJ)

11 - IGBT thermal resistance R_{thq} (j-c) : 0.104 (°C / W)

12 - Diode thermal resistance R_{thd} (j-c) : 0.2 (°C / W)

13 - Module case-heat sink thermal resistance Rth (c-f): 0.025 (°C / W)

14 - PWM switching frequency: 16 (KHz)

15 - Bus voltage : 680 (V)

16 - switching loss characteristic testing voltage V_{cc}: 600 (V)

17 - Motor terminal to terminal resistance: 0.0684 (ohms)

18 - Motor back EMF constant: 392 (V / KRPM)

19 - Motor terminal to terminal inductance: 1 (mH)

20 - number of motor poles : 32

21- Motor running speed : 500 (rpm)

22 - Motor peak phase current : 50 (A)

Outputs of Program:

Motor mean phase voltage (peak) $V_a = 116$ (Volts)

Motor phase back - EMF (peak) $V_f = 113$ (V)

Inverter PWM switching frequency : 16 (KHz)

Conduction loss per IGBT : 22 (W)

Switching loss per IGBT : 72 (W)

Conduction loss per Diode : 8 (W)

Reverse recovery loss per Diode : 10 (W)

Total losses per leg : 224 (W)

Inverter total power losses : 675 (W)

Inverter efficiency: 92 %

Inverter Output Power = 8615 W

IGBT junction - case temperature rise: 9.8 °C

Diode junction - case temperature rise: 3.6 °C

Module case - heatsink temperature rise: 5.6 °C

Junction Temperature = 125°C:

Input of Program:

1 - Power device part #: 2MBI150L - 120 (Fuji's 150 A 1200 V L Series IGBT)

2 - Motor #: B36 -152 - EBA - 26 (Motion Control Systems, Inc.)

3 - IGBT minimum V_{q0}: 2 (V)

4 - Device characteristics testing current I_{test}: 150 (A)

5 - IGBT voltage at the testing current V_q: 3.2 (V)

6 - Diode minimum V_{d0}: 0.9 (V)

7 - Diode forward voltage at the testing current V_d: 1.5 (V)

8 - IGBT turn - on switching loss E_{on} at I_{test}: 31.25 (mJ)

9 - IGBT turn - off switching loss E_{off} at I_{test}: 25.6 (mJ)

10 - Diode reverse recovery loss E_{rr} at I_{test}: 7.8 (mJ)

11 - IGBT thermal resistance R_{thq} (j-c) : 0.104 (°C / W)

12 - Diode thermal resistance R_{thd} (j-c) : 0.2 (°C / W)

13 - Module case-heat sink thermal resistance Rth (c-f): 0.025 (°C / W)

14 - PWM switching frequency: 16 (KHz)

15 - Bus voltage : 680 (V)

16 - switching loss characteristic testing voltage V_{cc}: 600 (V)

17 - Motor terminal to terminal resistance: 0.0684 (ohms)

18 - Motor back EMF constant: 392 (V / KRPM)

19 - Motor terminal to terminal inductance: 1 (mH)

20 - number of motor poles : 32

21- Motor running speed : 500 (rpm)

22 - Motor peak phase current : 50 (A)

Outputs of Program:

Motor mean phase voltage (peak) V_a = 116 (Volts)

Motor phase back - EMF (peak) V_f = 113 (V)

Inverter PWM switching frequency : 16 (KHz)

Conduction loss per IGBT : 23 (W)

Switching loss per IGBT : 109 (W)

Conduction loss per Diode : 6 (W)

Reverse recovery loss per Diode : 15 (W)

Total losses per leg : 306 (W)

Inverter total power losses : 922 (W)

Inverter efficiency: 90 %

Inverter Output Power = 8615 W

IGBT junction - case temperature rise: 13.7 °C

Diode junction - case temperature rise: 4.2 °C

Module case - heatsink temperature rise: 7.6 °C

Chapter 4

Experimental Verification

The model has been extensively verified in the laboratory. Inverter operating at different bus voltage (340 V and 680 V both DC) at different PWM frequencies (8 KHz to 16 KHz), different phase current levels (14 A to 120 A) at different mode of operation (motoring and stall). Some examples will be shown in the thesis.

4.1 Verification Method

Electrical power loss measurement of an inverter is difficult to do because the output voltages of the inverter are PWM waveform with large dv/dt. It takes very wide-bandwidth and noise interference-free wattmeter to measure the inverter output power accurately. This problem is compounded by the fact that both output voltage and output current are large in magnitude but the power input or output may be small i.e. very small effective power factor. Therefore, the verification of the model discussed above is done by using thermal measurement to be discussed in the following section. However, when the motor is at stalled mode, the electrical power measurement can be done accurately because of DC nature of the current flowing through phases, therefore the electrical

measurement was used to verify the theoretical results when the motor is operating at stalled condition.

4.2 Thermal Measurement of Power Dissipation

To verify the power losses by thermal measurement, the package of the inverter must be calibrated first. To calibrate a particular inverter-heat sink assembly, a known power dissipation to the device is created and temperature of the heat sink is measured as shown in Figure 4.1, IGBT-diode modules were mounted on a heat sink which can either be fan cooled or convection cooled. A DC power supply is used to supply a controllable current through the IGBTs which are purposely operated in active mode by proper gate drive voltage. Each of the six IGBTs is dissipating about the same amount of power. This condition is created to simulate the loss distribution while the motor is operating in a motoring mode in which average power losses are evenly distributed to all the six IGBTs-diode pairs. It should be noted that the same IGBT-diode modules are used in the calibration phase of the heat sink and in the actual inverter measurement so that there is no change in thermal system between calibrated measurement and an actual inverter. By measuring the temperature rise of the heat sink and the total power input, one can obtain a Power Losses vs. Heatsink Temperature characteristic curve which can later be used as a

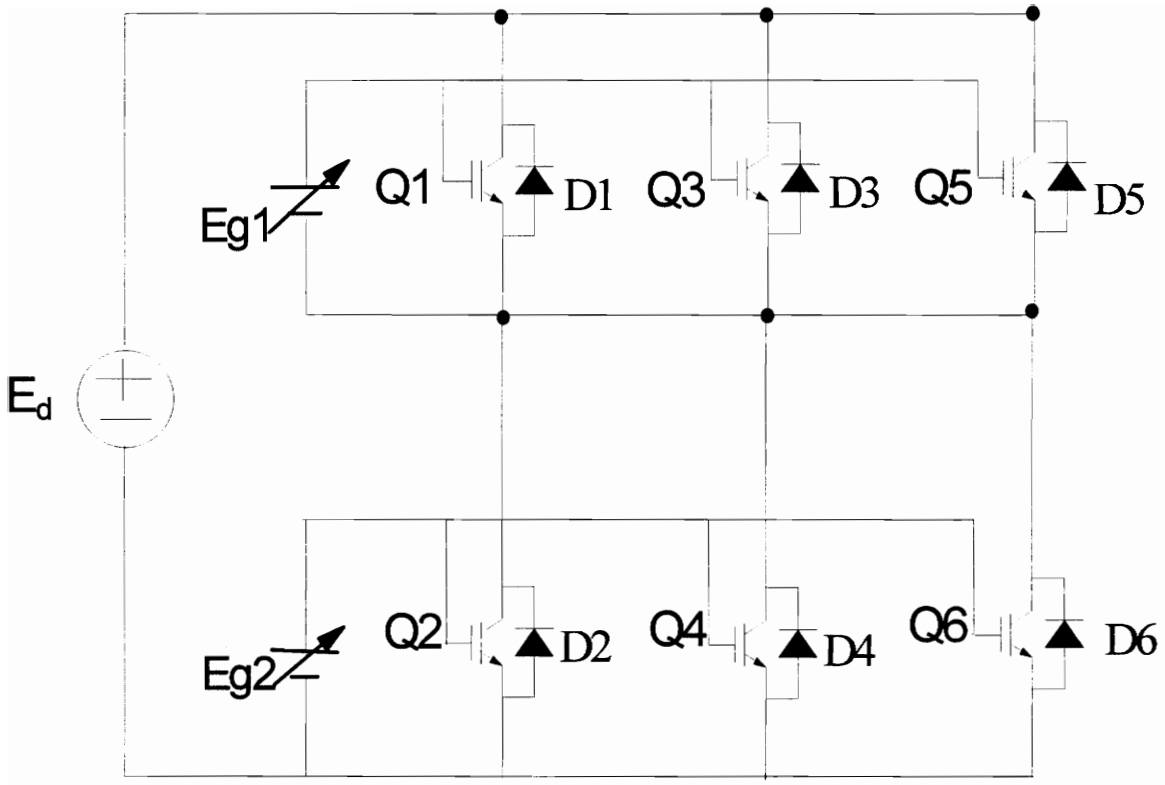

Fig. 4.1 Thermal Measurement of Power Losses

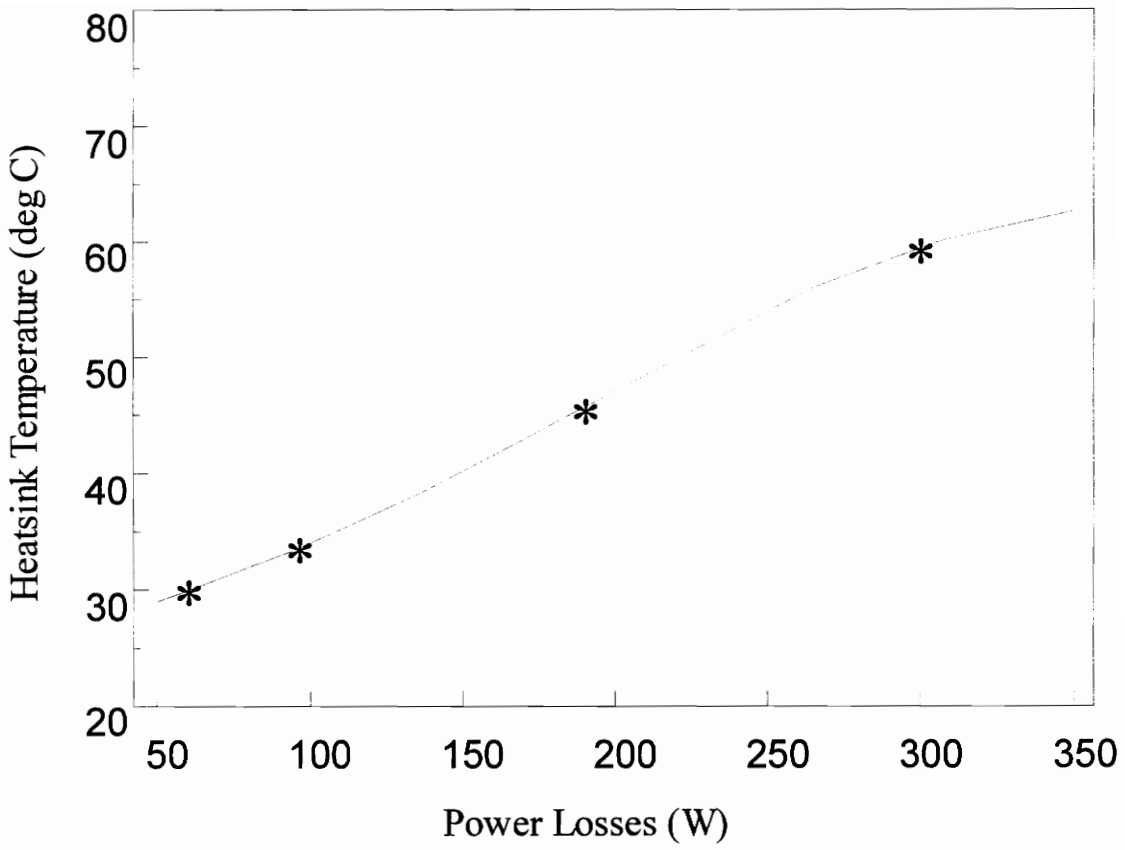

Ambient Temperature = 25 deg C
Heatsink Size = 8" x 9.875" x 1"
Fin Number = 30
Aluminum Heatsink with Fan Cooling
Temperature Measured at Midpoint of Heatsink

Fig. 4.2 Temperature vs. Power Losses for a Particular Heatsink (Heatsink # 1)

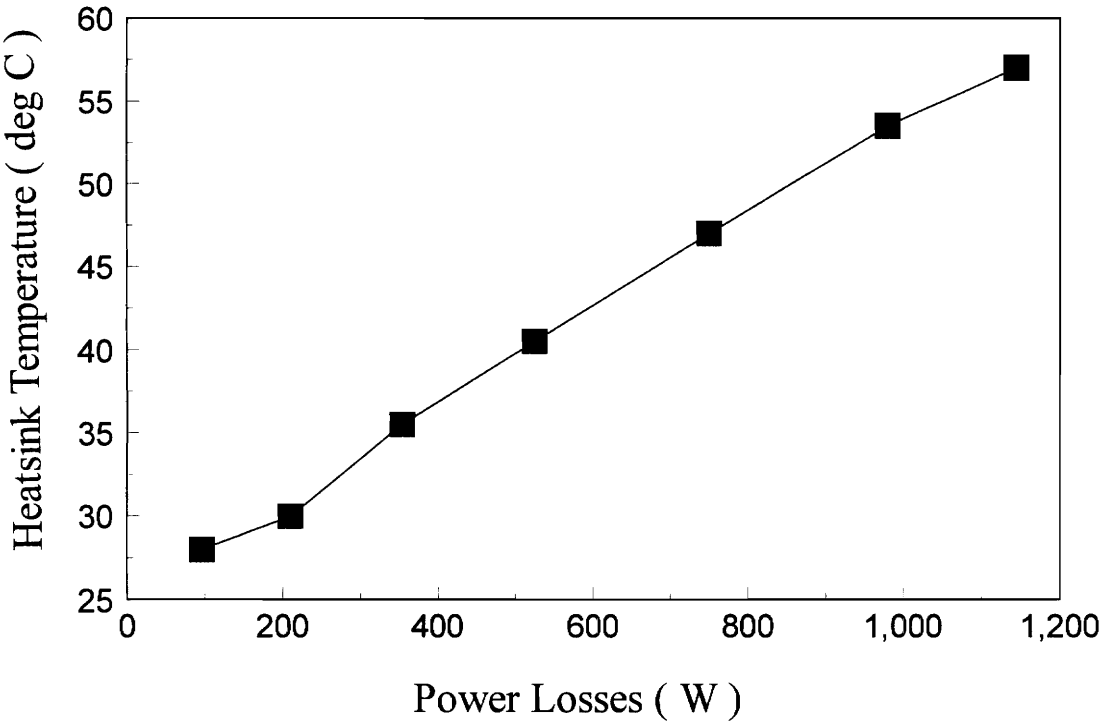

Ambient Temperature = 25 deg C
Heatsink Size = 14" x 9.75" x 1.985"
Fin Number = 20
Aluminum Heatsink with Fan Cooling
Temperature Measured at Midpoint of Heatsink

Fig. 4.3 Temperature vs. Power Losses a Particular Heatsink (Heatsink # 2)

reference for finding out the total inverter losses. Figure 4.2 shows an example of such curve of a particular thermal system in experiment. In this example, the testing condition is that the heat sink size is 8"× 9.875"×1" with 30 fins (fin mean thickness is 0.075") and the package is air blown by two fans as well as the ambient temperature of 25 C°.

The power dissipation of an actual inverter can be obtained by measuring the heat sink temperature (while the inverter is in operation) and by using Figure 4.2. For example, if the heat sink temperature is measured to be 40 C°, then the inverter power loss is approximately 120 W from Figure 4.2. It is noted that this figure is good only for a particular heat sink system. For each new thermal system, experiments must be conducted to obtain a new calibrated curve. Figure 4.3 shows another example of a curve of another particular thermal system in experiment. All testing conditions are indicated in the figure.

4.2.1 Verification of Motoring Mode Losses

Table 4.1, 4.2 and 4.3 show several examples of the calculated and the measured results. Both the measured and the calculated power losses were obtained by using the measured temperature of the heat sink and the Heatsink Temperature vs. Power Losses curve of Figure 4.2 and Figure 4.3 respectively. The measurement error is within 15 %.

Table 4.1. Power Loss Verification of Motoring Mode

(V_{bus} = 340V, Ambient Temperature = 25°C, For Heatsink #1 Information, See Fig. 4.2)

Peak Motor Phase Current		14 A	28 A
Heat sink temperature	Calculation	32°C (85 W)	41°C (153 W)
f_s = 8.5 KHz	Measurement	31°C (78 W)	39°C (140 W)
Heat sink temperature	Calculation	36°C (116 W)	50°C (221 W)
f_s = 16.2 KHz	Measurement	35°C (108 W)	48°C (206 W)

Power Device Module: Fuji's 2MBI150L-060 (150 A, 600 V) IGBT Dual Module

Table 4.2. Power Losses Verification of Motoring Mode

(V_{bus} = 340V, Ambient Temperature = 25 °C, For Heatsink #2 Information, See Fig. 4.3)

Peak Motor Phase Current		30 A	60 A	90 A	120 A
Heat sink temperature	Calculation	30°C (183 W)	36°C (373 W)	41°C (571 W)	47°C (776 W)
f_s = 8.5 KHz	Measurement	30°C (183 W)	35°C (346 W)	39°C (525 W)	45°C (713 W)
Heat sink temperature	Calculation	32°C (260 W)	40°C (528 W)	48°C (804 W)	56°C (1087 W)
f_s = 16.2 KHz	Measurement	31°C (228 W)	38°C (476 W)	47°C (763 W)	54°C (1013 W)

Power Device Module: Fuji's 2MBI300L-060 (300 A, 600 V) IGBT Dual Module

Table 4.3. Power Losses Verification of Motoring Mode

(V_{bus} = 680V, Ambient Temperature = 25°C, For Heatsink #2 Information, See Fig. 4.3)

Peak Motor Phase Current		25 A	50 A
Heat sink temperature	Calculation	33°C (282 W)	42°C (573 W)
f_s = 8.5 KHz	Measurement	32°C (258 W)	40°C (530 W)
Heat sink temperature	Calculation	38°C (457 W)	52°C (923 W)
f_s = 16.2 KHz	Measurement	37°C (425 W)	50°C (876 W)

Power Device Module: Fuji's 2MBI300L (300 A, 600 V) IGBT Dual Module

4.3 Electrical Measurement of Power Dissipation in Stalled Condition

In a stalled condition, the inverter power losses can be accurately calculated by measuring the input power and calculating the output power to the motor. The input power can be measured by using a voltmeter and a current meter. Since the motor is standing still, there is no lamination losses. Therefore, the inverter output power is equal to the winding loss of the motor which can be accurately calculated. Thus

Inverter loss (at stalled mode)

= Input power - Motor winding losses

$= V_1 \bullet I_1 - (I_A^2 \bullet R_A + I_B^2 \bullet R_B + I_C^2 \bullet R_C)$

4.3.1 Verification for Stalled Mode Loss

Table 4.4 and Table 4.5 show two examples of the comparison between the calculated and measured power losses in stalled mode. Extensive verification using this method has been conducted. Generally speaking, the measurement error is within 10%.

Table 4.4

Comparison of Inverter Power Losses between Calculated and Measured Results for Stalled Mode Operation

V_{bus} = 340 V, Fuji's 150 A,600 V L Series IGBT (2MBI150L-060)

Stalled Current: Ia, Ib, Ic (A)		14, 7, 7	28, 14, 14	42, 21, 21
P_{loss} (Watts) @	Calculation	65	134	215
f_s = 8.6 KHz	Measurement	63	137	214
P_{loss} (Watts) @	Calculation	90	178	280
f_s = 16.3 KHz	Measurement	88	174	279

Table 4.5

Comparison of Inverter Power Losses between Calculated and Measured Results for Stalled Mode Operation

V_{bus} = 156 V, Fuji's 150 A,600 V L Series IGBT (2MBI150L-060)

Ia, Ib, Ic (A)		10, 5, 5	20, 10, 10	30, 15, 15
P_{loss} (Watts) @	Calculation	32	71	115
fs = 8.6 KHz	Measurement	27	56	96
P_{loss} (Watts) @	Calculation	38	83	134
fs = 16.3 KHz	Measurement	35	77	113

Chapter 5

Evaluations of Existing IGBT Modules

Using the algorithm developed, investigations of existing IGBT modules has been conducted. Specifically, six investigations were commonly-asked questions about existing IGBTs working in a synchronous motor drive applications. The questions and the conclusions are summarized in the following.

Question #1: Does the stalled condition or the motoring condition limit the inverter current rating in a synchronous motor drive?

Conclusion: The total inverter power losses differ little between the low speed motoring mode and stalled mode of operation. In a motoring mode, the power losses distribute evenly among the six IGBT-diode modules. In a stalled mode, however, the losses are not evenly distributed. In the worst condition, one IGBT can have much larger temperature rise than the others. Figure 5.1 shows an example of the difference of junction temperature rise of an IGBT under two operating conditions, one for motor condition and the other the stalled condition. Notice the big difference in temperature rise between the two conditions. The net result is that a stalled operation limits the inverter current rating in a synchronous motor drive if PWM frequency is fixed. It should be noted that the

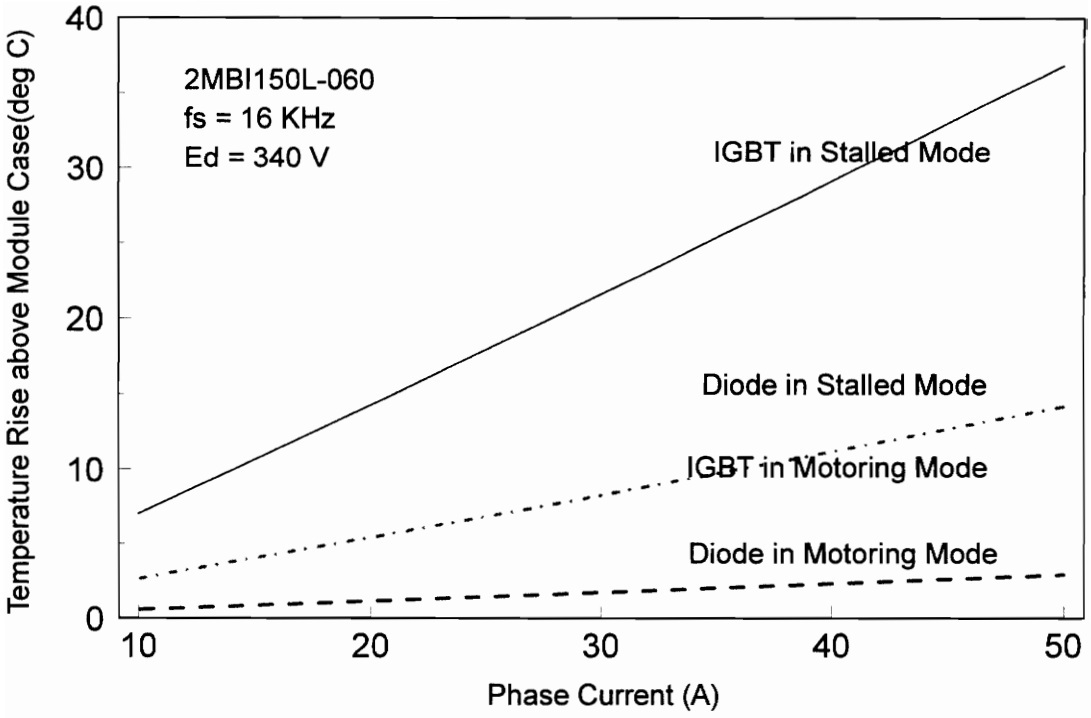

Fig 5.1 IGBT and Diode Junction to Case Temperature Rise

phenomenon of concentrated device heating does not happen in an induction motor drive system even in a stalled operation.

Question #2: What is the power losses distribution between IGBT and diode in motoring mode?

Conclusion: The power loss distribution between the IGBTs and the diodes depends on the particular module used, the motor operating condition and PWM frequency. In general, however, for the same motor current, the higher the motor speed, the higher the IGBT losses and the lower the diode losses. This is because the conduction duty cycle of IGBTs increases with speed but that of the diodes decreases. Figure 5.2 shows the power losses for different motor speed for a particular operating condition.

Question #3: It is stated in Conclusion #1 that, stalled operation limits the inverter rating because of concentrated heat. A question encountered often is " Is the IGBT or the diode the limitation ?"

Conclusion: An investigation of the commercial IGBT modules indicates that the limitation may lie in the IGBT or the diode, depending on the devices used and the switching frequency. Figure 5.3 shows the junction temperature rise of the diode and the IGBT for two different device types. As shown in the figure, for the Fuji's L-series IGBT, the IGBT is the limitation. For the N-series device, the IGBT is the limit for PWM

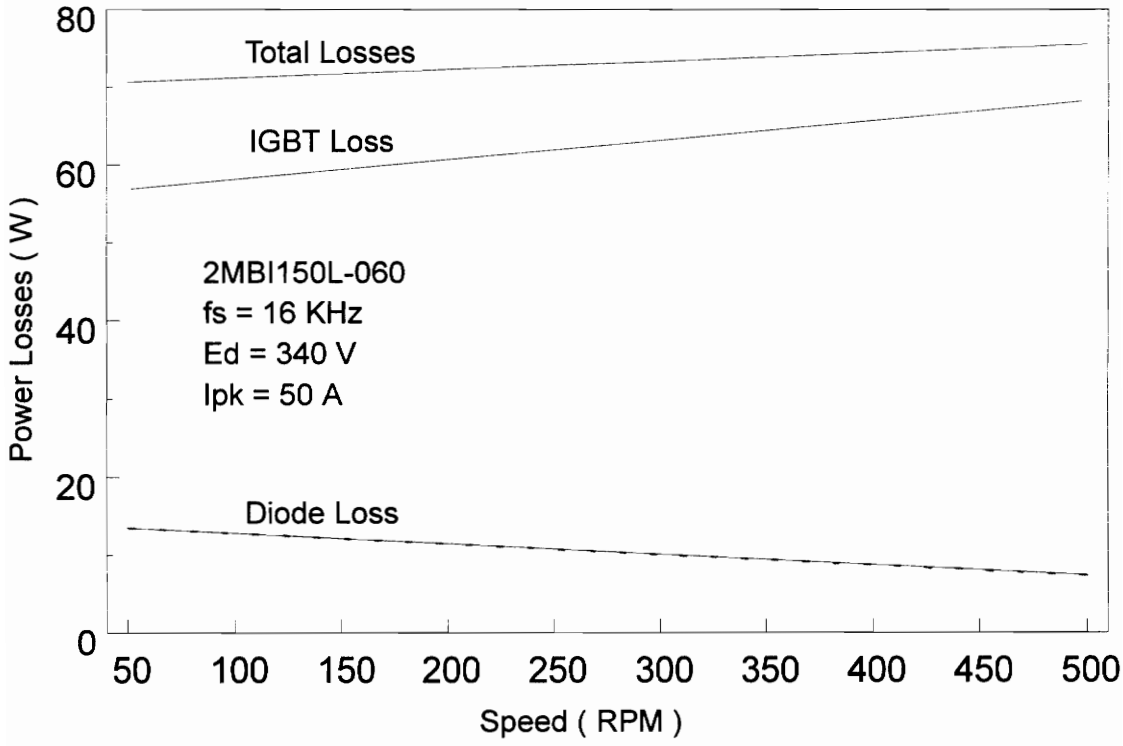

Fig. 5.2 Power Losses of IGBT and Diode in Motoring Mode

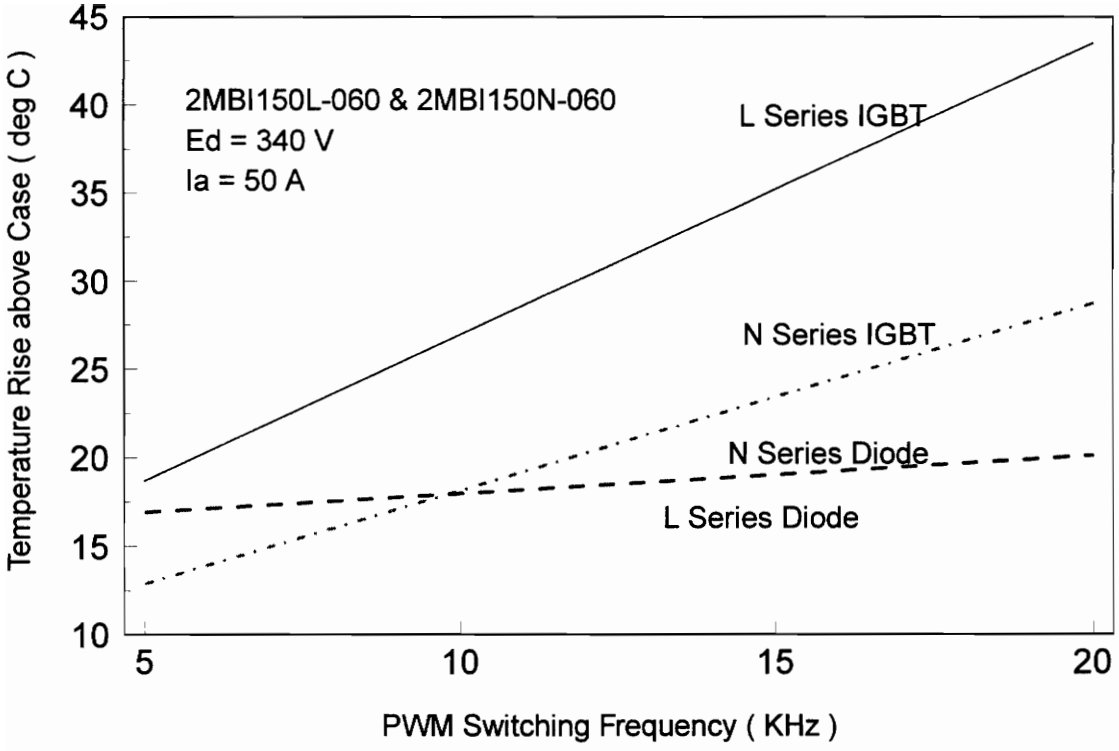

Fig. 5.3 IGBT and Diode Junction to Case Temperature Rise in Stalled Mode

frequency above 10 KHz and is otherwise for frequency below 10 KHz. Diode losses may be smaller than IGBT losses but because of larger thermal resistance associated with diodes, the temperature rise of diodes can be higher.

Question #4: What current derating factor should one use for IGBTs?

Conclusion: Based on a fixed temperature rise, at stalled mode, the current derating factor of a device varies with PWM frequency and can be calculated. Figure 5.4 shows an example of the proper derating factor for a commercial 600 V device operating at stalled mode. Take a PWM frequency of 16 KHz as an example, this figure shows that for this particular device (600V, 150A), the peak stalled current of inverter should be restricted to 67.5 A (a 45% derating) if the temperature rise (between junction and heat sink) is 40 °C. This is a very valuable information for device users.

Question #5: For high PWM frequencies (>20 KHz) and low voltage (< 200 V) applications, a MOSFET may be a more efficient device to use. However, IGBT provides large selection in terms of current rating. What is the possibility of using IGBT at high frequency?

Conclusion: Even with fast IGBTs (for example, Fuji's N series or Powerex's H series IGBTs), the switching losses still dominate the total power losses. Since the switching loss is essentially proportional to the bus voltage, an IGBT can be operated at far higher PWM frequency than suggested in the data sheet if the bus voltage is low.

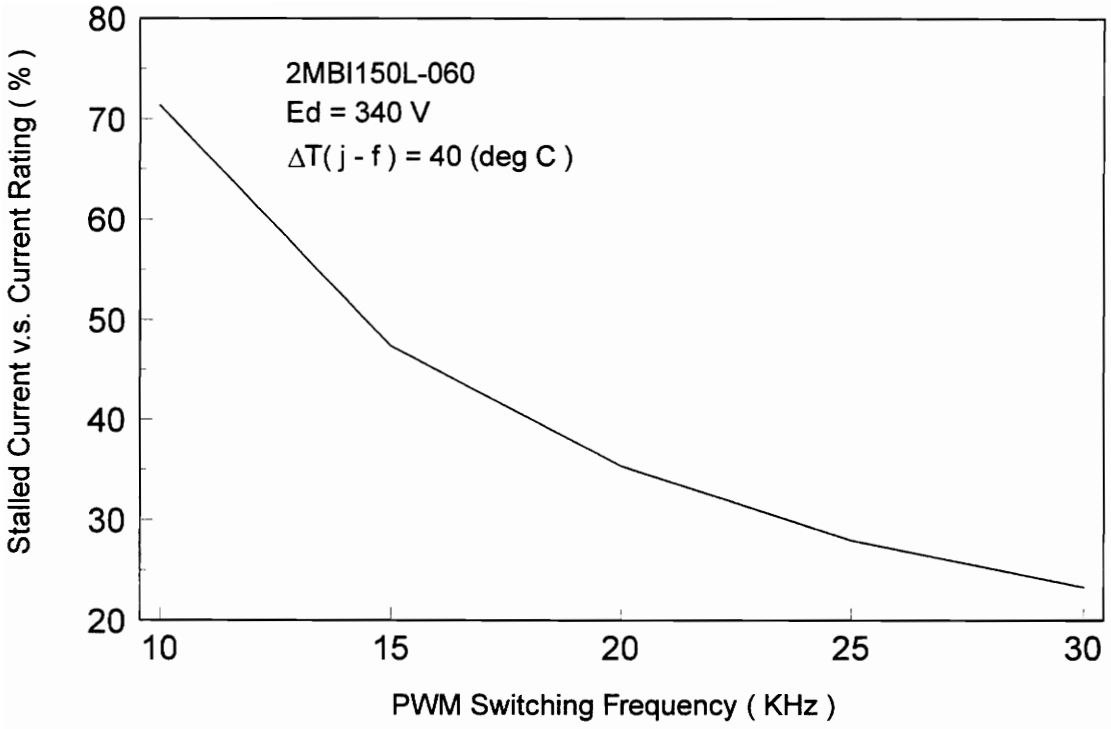

Fig. 5.4 An Example of Device Derating in Stalled Mode

Ideally, when the bus voltage is below 200 V and the PWM frequency is high, MOSFET is theoretically a better device to use. However, when the MOSFET selection is limited in terms of current, an IGBT is a good alternative.

Question #7: For the same output power, should one use high-voltage low-current approach or high-current low-voltage approach?

Conclusion: For the same speed and torque requirements with a motor, the output of the driving inverter is the same, and one has two options to choose either a high bus voltage inverter with a high inductance motor or a low bus voltage inverter with a low inductance motor. The high inductance motor has high back EMF constant and vice versa. Here are two examples (see Table 5.1 (a) and (b)) to show the comparison for two options. To fairly compare the two options, the bus voltage of the high bus voltage inverter and the back EMF of the high inductance motor are chosen twice as large as those of low voltage inverter and low inductance motor. It can be seen from Table 5.1 that high voltage low current system is not always better in efficiency. When the PWM frequency moves lower, the power losses is in favor of high voltage approach.

Table 5.1 (a)

Power device *	2MBI150L-120 (1200 V, 150 A)	2MBI300L-060 (600 V, 300 A)
Inverter bus voltage	680 V	340 V
PWM switching frequency	16 KHz	16 KHz
Motor model	A	B
Motor winding resistance	.0684 (ohm)	.0171 (ohm)
Motor winding inducdance	1 (mh)	.26 (mh)
Motor back emf constant:	392 (v/krpm)	196 (v/krpm)
Motor speed	500 (rpm)	500 (rpm)
Phase peak current	50 (A)	100 (A)
IGBT conduction loss	22 (W)	41 (W)
IGBT switching losses	120 (W)	92 (W)
Diode conduction loss	8 (W)	16 (W)
Diode reverse recovery loss	15 (W)	12 (W)
Inverter toal losses	993 (W)	967 (W)
Inverter output power	8487 (W)	8487 (W)
Inverter efficiency	89.5 %	89.7 %
IGBT junction to case temperature rise	15 (C°)	14 (C°)
Diode junction to case temperature rise	5 (C°)	6 (C°)
Module case to heat sink temperature rise	4 (C°)	4 (C°)

* Fuji' s L series IGBT dual module

Table 5.1 (b)

Power device *	2MBI75N-120 (1200 V, 75 A)	2MBI150N-060 (600 V, 150 A)
Inverter bus voltage	680 V	340 V
PWM switching frequency	16 KHz	16 KHz
Motor model	A	B
Motor winding resistance	.0684 (ohm)	.0171 (ohm)
Motor winding inducdance	1 (mh)	.26 (mh)
Motor back emf constant:	392 (v/krpm)	196 (v/krpm)
Motor speed	500 (rpm)	500 (rpm)
Phase peak current	25 (A)	50 (A)
IGBT conduction loss	8 (W)	15 (W)
IGBT switching losses	42 (W)	15 (W)
Diode conduction loss	3 (W)	7 (W)
Diode reverse recovery loss	10 (W)	2 (W)
Inverter toal losses	379 (W)	237 (W)
Inverter output power	4243 (W)	4243 (W)
Inverter efficiency	91.7 %	94.7 %
IGBT junction to case temperature rise	11 (C°)	6 (C°)
Diode junction to case temperature rise	6 (C°)	4 (C°)
Module case to heat sink temperature rise	3 (C°)	2 (C°)

* Fuji's N series IGBT module

Chapter 6

Conclusion and Recommendations for Future Study

6.1 Conclusions

A computer-aided tool is developed for predicting the power losses and the device temperature rise of an IGBT-based voltage-fed hard-switching DC-to-three phase inverter drive for synchronous motors. Three modes of motor operation are considered: motoring mode, regeneration mode and stalled mode. From a given set of semiconductor device parameter values, motor parameter values and motor operating conditions, one would be able to predict the various power losses associated with the inverter and the device temperature rise above the ambient. This facilitates inverter heat sink design and device module selection. The accuracy of the tool has been verified experimentally for a wide range of device rating.

Using this tool, a number of IGBTs were evaluated for the suitability of synchronous motor applications. Conclusions of this evaluation are presented in the thesis.

6.2 Recommendations for Future Study

1. Temperature effect on semiconductor device parameters are not incorporated in the present model. Parameter values at only two temperature (25 °C and 125°C) are available from manufacturer's data sheet. It is possible in the future to incorporate theoretical relationship between device parameter values and temperature into the model.

2. The device model can also be extended to include other devices such as MOSFETs and GTOs. However, switching loss data for these two devices are normally not given in data sheet. Effort is required to establish the data bank.

3. Sinewave modulation scheme is commonly used and is used in the present consideration. Space vector modulation[10] is gaining popularity and should be considered for extending the present capability of the tool.

4. Soft-switching inverter are gaining attention in recent years[11]. It should be possible to extend the present capability to include soft-switching inverters. Effort is required to establish the switching loss data of devices.

References

[1] B.K. Bose, *Power Electronics and AC Drives*, Prentice Hall, 1986

[2] Peter Vas. *Vector Control of AC Machines*, Clarendon Press, Oxford, 1990

[3] Ned Mohan, Tore M. Undeland and Wolliam P. Roobbins, *Power Electronics: Converters, Applications, and Design*, John Wiley & Sons, 1989

[4] J. Zubek, A. Abbondanti, and C. J. Nordby, "Pulsewidth Modulated Inverter Motor Drives with Improved Modulation," *IEEE Transactions on Industry Applications*, November/December 1975

[5] Robert W. Young, Sr., Jih-Sheng Lai, G. W. Ott, Jr., C. P. White, D. J. Adams, J. W. McKeever, and J. Milton Bailey, "Calculation of the Required Heat Sink Thermal Resistance of a Three-Phase SPWM Inverter Driving an Induction Motor," *Southcon 94 Conference Record*

[6] IGBT Data Book, Fuji Electric, October, 1992

[7] N-Series IGBT Specifications, Fuji Electric, October, 1994

[8] GTR Module (IGBT) Data Book, Toshiba Corporation Semiconductor Group, 1992

[9] IGBT and Intellimod^{TM} - Intelligent Power Modules Applications and Technical Data book, Powerex, October, 1994

[10] P. G Handley and J. T. Boys, "Space Vector Modulation: An Engineering Review," *4th International Conference on Power Electronics and Variable Speed Drive*, July 1990

[11] H. Mao and F. C. Lee, "Improved Zero-Voltage-Transition 3-Phase PWM Voltage Link Converter," *12th VPEC Seminar*, September 1994

Appendix

Glossary of Symbols

dD_m : Duty cycle of diode in motoring mode.

dQ_m : Duty cycle of IGBT in motoring mode.

dD_s : Duty cycle of diode at stalled mode.

dQ_s : Duty cycle of IGBT at stalled mode.

E_d (V_{bus}): Inverter input DC voltage source.

EQ_{on} : IGBT turn-on loss per switching cycle.

EQ_{off} : IGBT turn-off loss per switching cycle.

ED_{rr} : Diode reverse recovery loss per switching cycle.

f_s : PWM switching frequency.

I_a, I_b, I_c : Motor phase current.

i_a^*, i_b^*, i_c^* : Controller three phase current request.

I_{CE} : IGBT forward current.

I_D : Diode forward current.

I_{pk} : Peak phase current in motoring mode.

L_s : Motor phase winding inductance.

m : PWM modulation index.

pQ_c: IGBT average conduction loss per switching cycle in motoring mode.

pD_c : Diode average conduction loss per switching cycle in motoring mode.

PQm_c : IGBT average conduction loss in motoring mode.

PDm_c : Diode average conduction loss in motoring mode.

PQm_{on} : IGBT average turn-on loss in motoring mode.

PQm_{off} : IGBT average turn-off loss in motoring mode.

PDm_{rr} : Diode average reverse recovery loss in motoring mode.

PQs_c : IGBT conduction loss at stalled mode

PDs_c : Diode conduction loss at stalled mode

PQs_{on} : IGBT turn-on loss at stalled mode.

PQs_{off} : IGBT turn-off loss at stalled mode.

PDs_{rr} : Diode reverse recovery loss at stalled mode.

R_Q : IGBT on resistance.

R_D : Diode on resistance.

R_s : Motor phase winding resistance.

V_a : Phase voltage with respect to the center point of E_d.

V_{a1} : The fundamental of V_a.

V_{CE} : IGBT collector-emitter voltage.

V_{CE0} : IGBT collector-emitter voltage at $I_{CE} \approx 0$.

V_D : Diode forward voltage.

V_{D0} : Diode forward voltage at $I_D \approx 0$.

V_f : Motor back-emf voltage.

V_{ref} : Current error signal.

V_t : Triangular carrier voltage for generating PWM switching.

V_{test} : DC bus voltage from switching energy data sheet.

ω : Motor stator angular frequency.

ω^* : Controller speed request.

φ : Phase angle between V_{al} and I_a.

ψ_f : Motor rotor field flux.

Vita

Jian Yang was born in Changsha, Hunan, People's Republic of China (P. R. China) on April 4, 1959. He graduated from Changsha 6th High School in Changsha, P. R. China in 1977.

He received his Bachelor of Science degree in electrical engineering from Hunan University, P. R. China in January 1982. From March 1982 to November 1983, he was employed as an electrical design engineer at Changsha Motor Factory. In December 1983, he transferred to Changsha University. While working as a Lecturer at Changsha University from 1983 to 1992, he came to the Virginia Power Electronics Center (VPEC) at Virginia Polytechnic Institute and State University to study and do research work as a visiting scholar from 1986 to 1987.

In August 1992, he joined VPEC at Virginia Polytechnic Institute and State University again as a graduate student. While studying at VPEC, he was employed at Motion Control Systems, Inc. to do research and development work. In September 1995, he completed the requirements for the Master of Science degree.

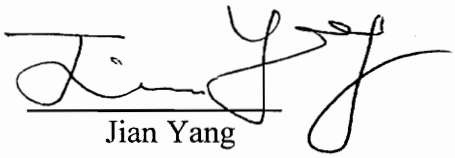

Jian Yang